NON- DRIVEN ACCUMULATOR ROLL ANALYSIS USING THE FINITE ELEMENT METHOD

by

Hazel M. Pierson

Submitted in Partial Fulfillment of the Requirements

for the Degree of

Master of Science

in the

Mechanical Engineering

Program

YOUNGSTOWN STATE UNIVERSITY

August, 1998

NON- DRIVEN ACCUMULATOR

ROLL ANALYSIS USING THE

FINITE ELEMENT METHOD

by

Hazel M. Pierson

I hereby release this thesis to the public. I understand this thesis will be housed at the Circulation Desk of the University library and will be available for public access. I also authorize the University or other individuals to make copies of this thesis as needed for scholarly research.

Signature:

Hazel M. Pierson — 8-4-98
Student — Date

Approvals:

Thesis Advisor — 8/4/98 — Date

Committee Member — 8-4-98 — Date

Committee Member — 8/4/98 — Date

Dean of Graduate Studies — 8/14/98 — Date

ABSTRACT

The purpose of this study was to develop a method to analyze various designs of accumulator rolls using a static finite element software package. This would allow the engineer to determine how the various components of the roll design contribute to or lessen the deflection of and stresses in the roll body when it is loaded by sheet metal passing over or under it. The method outlined is intended mainly for use when an advanced dynamic finite element package that incorporates contact elements is not available and when a comparison of various roll designs is desired.

First, an approximation of the pressure on the roll body caused by the force of the sheet metal as it wrapped over or under the roll was determined. Then using the finite element package ALGOR, an FEA model of a standard accumulator roll design was loaded with this pressure and the stresses and deflections were calculated. Next, components of this basic roll design were varied in the FEA model. These were the location of the stiffeners and the thickness of the roll body, the end plates, and the stiffeners. A comparative approach was then used to assess the impact each of these variations in roll design had on the deflection of and the stresses in the roll.

ACKNOWLEDGMENTS

Dr. Daniel H. Suchora - Thesis Advisor

Dr. H. W. Kim - Thesis Committee

Dr. Robert A. McCoy - Thesis Committee

Anthony Viviano - Figures and Technical Support

To Kris, Matt, and Emma

TABLE OF CONTENTS

LIST OF FIGURES

LIST OF TABLES

CHAPTER 1

INTRODUCTION

1.1 BACKGROUND

Steel and aluminum industries, because of the competition inherent in most primary product industries, need dependable equipment to meet ever-increasing production and quality standards. In order to meet and surpass these standards, in as efficient and cost effective manner as possible, rolling mill design companies, suppliers, and manufacturers must continually evaluate and improve equipment through research and development. Frequently it means taking a new look at various components of equipment that were designed with "trial and error" techniques to determine if a more cost-effective design could work just as well or even better. [1] This has become feasible because advanced stress analysis techniques, particularly finite element analysis, can now be used to conduct a more thorough analysis of complex equipment components, thus narrowing the number of viable options before any "trial" stage is performed.

One such area in which finite element analysis proves to be a useful tool for design evaluation is in the determination of deflections and stresses present in

accumulator and deflector rolls during strip metal operations such as the annealing line shown in Figure 1.1.

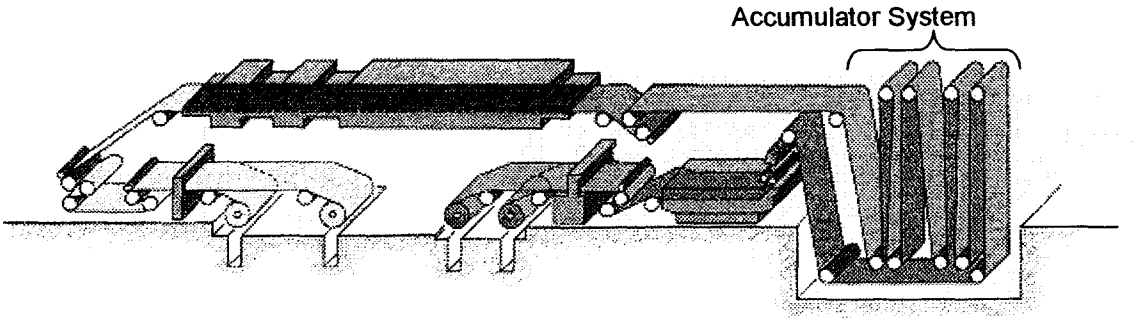

FIGURE 1.1 Annealing processing line with accumulator system

Nearly all coil strip metal processing mills have a system of vertically or horizontally mounted accumulator rolls in their various processing lines. This is important for production since the accumulator system allows portions of the processing line to continue running when other portions must be temporarily stopped. An example of this for the annealing line shown above would be during strip metal coil changes. The annealing process can continue without interruption, fed by the strip that was built up in the accumulator system, while a new coil of strip metal is installed and welded to the end of the previous coil. Once the new coil is in place the portion of the line that had to be stopped can restart and the accumulator system can begin to re-accumulate strip for the next time. Therefore, down time due to necessary maintenance procedures is eliminated and loss of processed material due to complete re-threading of a new strip is alleviated.

The design of the accumulator rolls has basically been the same for many years because once a tried and true design was found there was little reason to chance a design change. However, as stated before, considering the vast amount of accumulator rolls that are used in processing lines, especially the newer lines that perform multiple processes, economic considerations have now provided the fuel to consider a thorough design evaluation.

1.2 SOFTWARE CONSIDERATIONS

There are computer programs available for optimizing an accumulator roll design based on the geometry and loading conditions of the sheet metal it is to accumulate. However, these programs have historically been unreliable since they seem to be based largely on extreme simplifying assumptions similar to hand calculations. Now with the emergence of finite element analysis, a more thorough way to evaluate a roll design change is possible. In fact, solutions to dynamic, contact surface problems, such as the accumulator roll, are becoming easier to obtain with the advanced technology available from computers and highly sophisticated finite element software packages. Still, the software packages capable of this advanced non-linear analysis require more computing power than is readily available on an average personal computer. Also, a full scale finite element analysis may not be practical for the engineer who simply needs to first qualitatively see the effect varying one parameter of the roll design has on the deflections of and the stresses in the roll. For these reasons, simplifying assumptions are made in this analysis of accumulator roll designs as

a first look at exploring the benefits the finite element technique has to offer while keeping it practical to the average engineer. This will be discussed in the following chapter.

Therefore, keeping this in mind, a three dimensional analysis of the finite element model of a standard accumulator roll is performed. Several components of the roll are then varied and the finite element model of these design alternatives are analyzed in the same manner. A comparative approach is then used to assess the impact each of these variations in roll design has on the deflection of and the stresses in the roll. Perhaps this will help take the doubt out of the old design standard of "when in doubt, build it stout."

CHAPTER 2

DESIGN CONSIDERATIONS

2.1 ROLL CONSTRUCTION

The standard accumulator roll consists of a roll shell or body, roll stiffeners, end plates and hubs, and a roll shaft. Figure 2.1 shows a cut-away view of this.

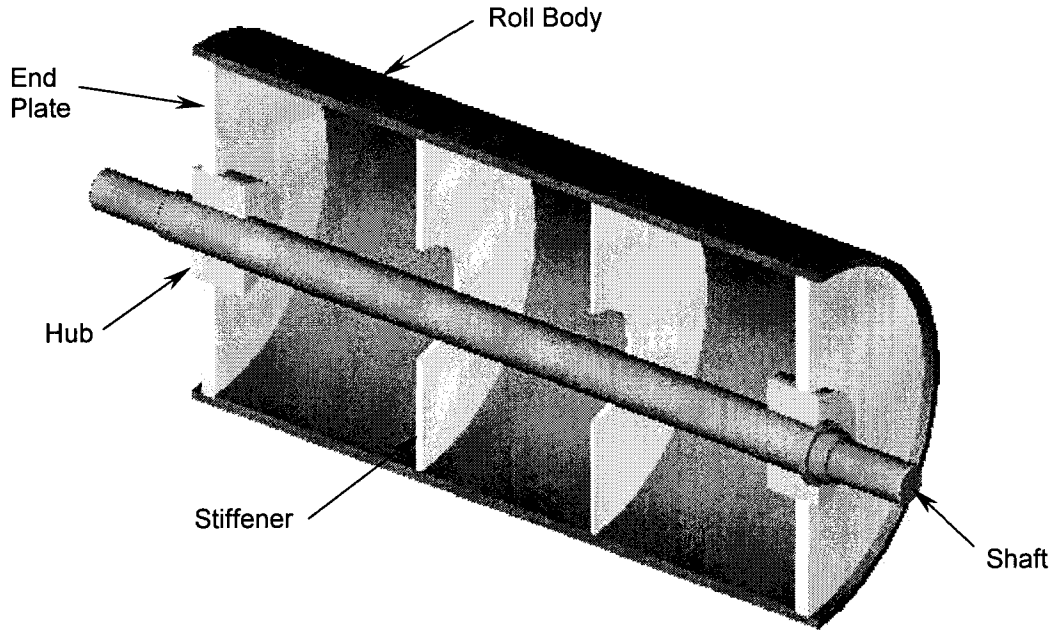

FIGURE 2.1 3-D cut-away view of an accumulator roll

The roll stiffeners are transverse welded disks commonly recommended to help maintain a near perfect cylinder when a welded steel roll with an outer shell, such

as an accumulator roll, is loaded. [2] These are placed intermittently within the roll body and are welded to it along with the end plates. The hubs are welded on to the end plates and the shaft is press fit into the hubs. There is a wide range of accumulator roll dimensions available, dependent upon the sheet metal size and type the roll is to accumulate. The roll chosen for analysis in this investigation was provided as a "typical" accumulator roll from an actual roll manufacturer. The roll has an overall roll body length of 60" and thickness of 1". The outside diameter of the roll body was 32". The end plates were 1¼" thick and the stiffeners were ½" thick, both with an inside diameter of 10". The hubs were 5" in length and had an outside diameter of 10" and an inside diameter of approximately 4". The shaft was secured with bearings whose center lines were 6" from the end of the roll. It was approximately 4" in diameter and 77½" long. Both the shaft and roll body were formed from 1045 steel. The rest of the components of the roll were formed from 1018/1020 steel. A drawing of this roll is located in Figure A.1 of the appendix.

2.2 ASSUMPTIONS

As was mentioned previously, simplifying assumptions were made in this analysis of accumulator roll designs as a first look at exploring the benefits the finite element technique has to offer while keeping it practical to the average engineer. Firstly, although accumulator roll functioning is obviously dynamic, the roll was modeled as a stationary roll, held on either side of the shaft with bearing supports. Because the accumulator rolls are non-driven idler rolls, the tension in

the strip metal rolling over or under them is approximately the same on either side of the roll when the line reaches a steady state condition. Even at other times when the line is not at steady state, for example during line start up or shut down, the variation in the tension applied to the strip from one side of the roll to the other is assumed to be negligible. Therefore, as long as it is recognized that fatigue effects of the spinning roll and shaft are not being addressed, a stationary roll is a valid approximation.

Secondly, the load that is transferred from the strip to the roll because of the tension in the strip metal was approximated as a uniform pressure distribution on the roll in the radial and longitudinal direction. This was a necessary simplifying assumption because of the limited capabilities of the finite element package that was used in the analysis. There were no adequate contact elements available that would allow the software to simulate the transfer and distribution of the load from the strip metal to the roll. It was reasoned that a uniform pressure would be a worst case scenario since it was thought that if the distribution was non-uniform, the stiffer portions of the roll would take more of the load than the weaker portions. This would result in the roll body actually having less deflection than an analysis using uniform pressure distribution would show. Therefore, this assumption leads to a conservative approach of appropriate roll designs since the determined roll body deflections and stresses will be more than in actuality. The determination of an appropriate pressure value is addressed in a subsequent chapter.

Thirdly, limitations were placed on the components and parameters of the roll that would be varied in this research. Because this is a first look at a finite element analysis of an accumulator roll, previous information concerning roll design in general was considered to help narrow the alternative design options. For example, there is a readily available supply of information concerning the necessary outer dimensions of accumulator rolls for a given range of sheet metal thickness. Development of a standard for this was necessary in order to assure certain ill effects such as coil set and cross bow did not occur in the strip metal. [3,4] Also, ASME codes are available to determine the required roll shaft diameter of a roll for a given load and torque rating. [5] Because of this, it was decided to vary neither the outside diameter of the roll body nor the diameter of the shaft in this analysis. Therefore, the focus of this research was more on the parts of the roll that designers have the most leeway when designing; the parts that lend themselves to a finite element evaluation for design optimization: the roll body keeping the outside diameter constant, the roll stiffeners, and the end plates. The variation of these roll components will be discussed later.

2.3 DATA INTERPRETATION

Because of these basic assumptions, the significance of the finite element evaluation of this research is in the comparative aspect of design optimization. Therefore, the stress and deflection values for each individual roll design in this finite element analysis are not meant to be used as a true determination of the

values present when the roll is in use. On the contrary, when simplifying assumptions are made, the actual values lose their meaning and one must be careful when drawing conclusions based on them. However, the stress and deflection profiles of the standard roll, described in section 2.1, when compared to the profiles of rolls that had one or more of the component parameters varied, took on a qualitative significance in their interpretation. This is because it is reasoned that the trend in the stress and deflection profiles and values as a component of the roll is varied would be indicative of the actual trend that would be observed when the roll is in use. Therefore it is from this qualitative point of view that the results were interpreted.

CHAPTER 3

ELEMENT FORMULATION

3.1 OVERVIEW

The finite element analysis was done using the FEA software program ALGOR. [6] Three different types of elements in the program were used to model the roll assembly: Type 2 beam elements, Type 5 solid elastic brick elements, and Type 6 plate/shell elements. [7] The type of element chosen to model a certain portion of any assembly depends on a variety of factors. In this analysis, consideration was given to geometrical size of a component and its function within the assembly as well as to realistic computer program execution times. The elements were combined together to create the full model.

3.2 BEAM ELEMENTS

The Type 2 beam elements are three-node elements formulated in three-dimensional space. Two nodes (I and J) designate the length of the beam and the third node (K) is used to arbitrarily orient each beam element in 3-D space. Figure 3.1 shows the orientation of a typical beam element.

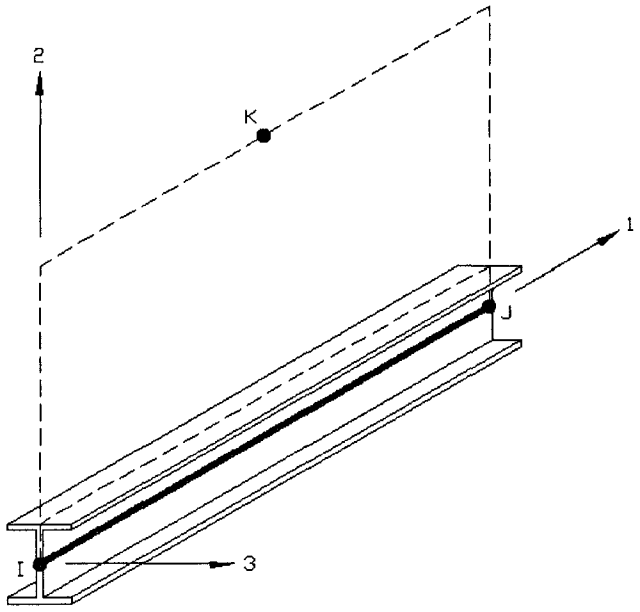

FIGURE 3.1 Type 2 beam element orientation in 3-D space

The element has six degrees-of-freedom at each node. These include translations in the x, y, and z-directions and rotations about the nodal x, y, and z-axes. Area property data and material property data also define the beam. The area property data consists of axial or cross-sectional area, shear areas, torsional resistance, flexural moments of inertia, and section moduli. The material property data includes the modulus of elasticity, Poisson's ratio, mass and weight density, thermal expansion coefficients, and stress free reference temperature. It is a uniaxial element with tension, compression, torsion, and bending capabilities. Uniform inertia loads in three directions, fixed end nodal forces, and intermediate loads are the basic element loadings. Figure 3.2 shows a beam element with its degrees-of-freedom.

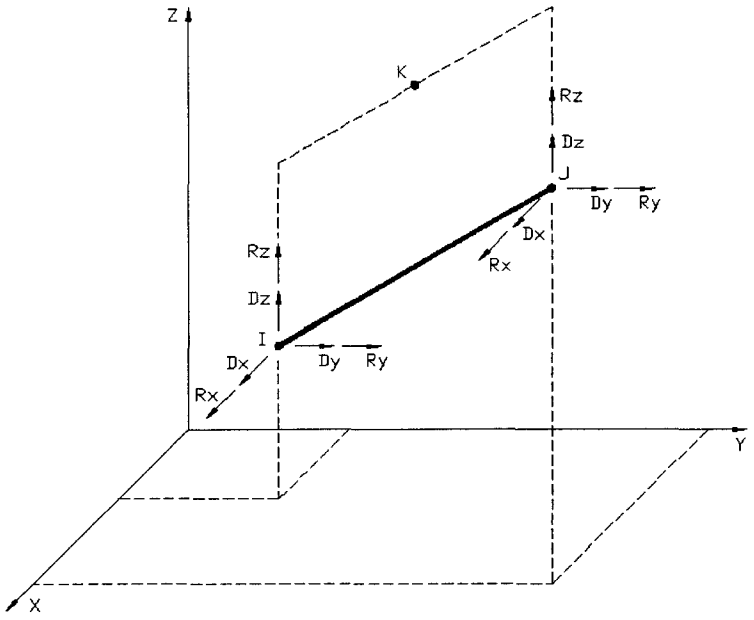

FIGURE 3.2 Type 2 beam element with degrees-of-freedom

3.3 BRICK ELEMENTS

The Type 5 three-dimensional, solid elasticity brick elements are four to eight-node elements formulated in three-dimensional space. The element has only three degrees-of-freedom defined at each node: translations in the x, y, and z-directions. The elements used in this study were six and eight-node bricks. Material properties are assumed to be isotropic with the data including the modulus of elasticity, Poisson's ratio, weight density, thermal expansion coefficients, and the shear modulus. Fixed end nodal forces, pressure, thermal, and uniform inertia loads in three directions are the allowable element loadings. Figure 3.3 shows an eight-node brick element with its degrees-of-freedom. The six-node brick elements are similar but triangular in shape.

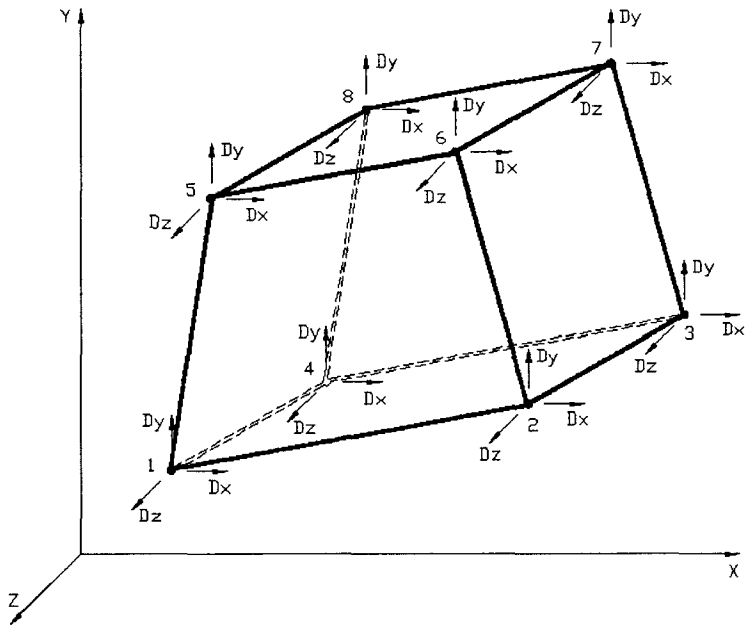

FIGURE 3.3 Type 5 eight-node solid elasticity brick element with degrees-of-freedom

3.4 PLATE ELEMENTS

The Type 6 plate or shell elements are three or four-node elements formulated in three-dimensional space. These elements have five degrees-of-freedom: translations in the x, y, and z-directions and two rotations that produce out-of-plane bending. The rotation normal to the plane of the plate is not defined. Material properties can be anisotropic. However, the material property data must produce a positive definite stress-strain matrix. Element property data and material property data define the plate element. Element data includes element thickness, distributed lateral pressure, mean temperature variation, and through thickness variation. The material property data consists of elastic constant data such as modulus of elasticity, Poisson's ratio, and shear modulus as well as

control data such as weight and mass density and thermal expansion coefficients. Fixed end nodal forces, pressure, thermal, and uniform inertial loads in three directions are the allowable element loadings. Stress output includes in-plane membrane stresses and out-of-plane bending stresses. Figure 3.4 shows a four-node plate element with its degrees-of-freedom. The three-node plate elements are similar but with a triangular shape.

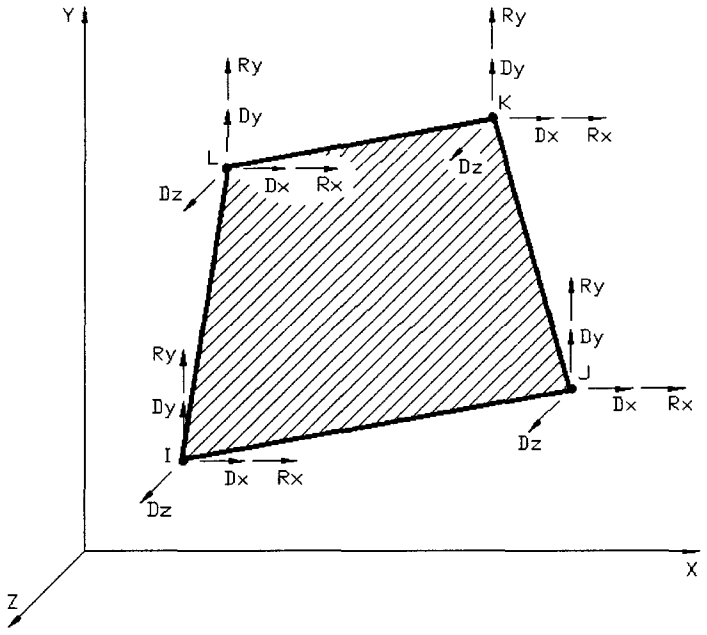

FIGURE 3.4 Type 6 four-node plate or shell element with degrees-of-freedom

CHAPTER 4

THE FINITE ELEMENT MODEL

4.1 MODELING TECHNIQUE

The finite element model used in this study needed to take into account two separate parts; the non-driven (no torque input) accumulator roll and the strip metal that rolls over it. Because of the symmetrical geometry of the roll assembly, shaft, and strip metal there are two planes of symmetry in the finite element model. A typical accumulator roll is shown in Figure 4.1.

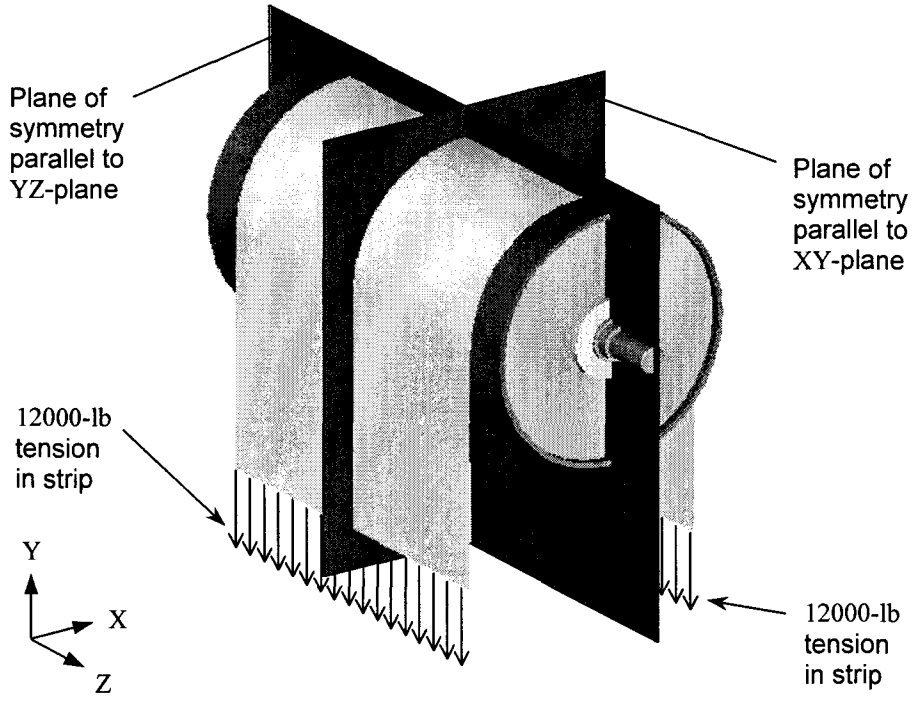

FIGURE 4.1 Planes of symmetry in a typical accumulator roll

Referring to the above figure, longitudinal symmetry is depicted in the XY-plane and circumferential symmetry in the YZ-plane of a typical accumulator roll that has a 180° wrap of strip metal.

Because of the symmetry, the analysis was simplified to that of a one-quarter model of the full assembly, shown in Figure 4.2. This is done by constraining the nodes on the lines of symmetry of the finite element model in such a way as to simulate the evaluation of a full model. Doing this facilitates a more accurate model, since a finer finite element mesh could be used, while still reaping the benefit of a reduced program execution time.

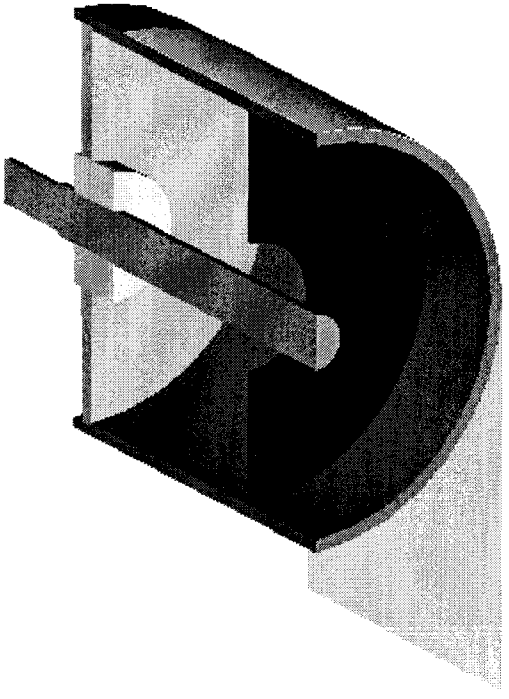

FIGURE 4.2 One-quarter of a fully assembled accumulator roll

The accumulator roll was modeled with the three different types of finite elements discussed in Chapter 3. The roll shaft was modeled using the Type 2 beam elements. Referring to Figure 4.3, the circled nodes are the nodes that are

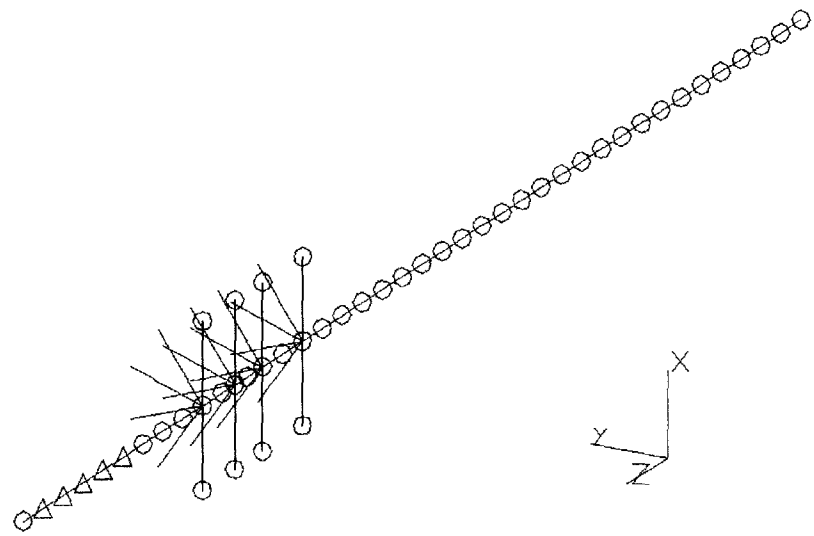

FIGURE 4.3 Roll shaft modeled with beam elements

constrained with symmetry boundary conditions. The nodes with triangles have boundary conditions that are consistent with constraint by the shaft bearing. The beam elements that flange out from the beam elements of the shaft are used only to tie the shaft to the hub. This is necessary because there are no physical dimensions in the radial direction of the beam elements although the finite element solver recognizes the inputted dimensions of the shaft when performing the analysis. These linking beam elements were given a very high modulus of

elasticity (stiffness) to accomplish this purpose and to simulate the stiffness of the shaft where it joins the hub.

The hub and end plates of the roll body were modeled using the Type 5 solid elasticity brick elements, shown in Figure 4.4. Again, the circles show the

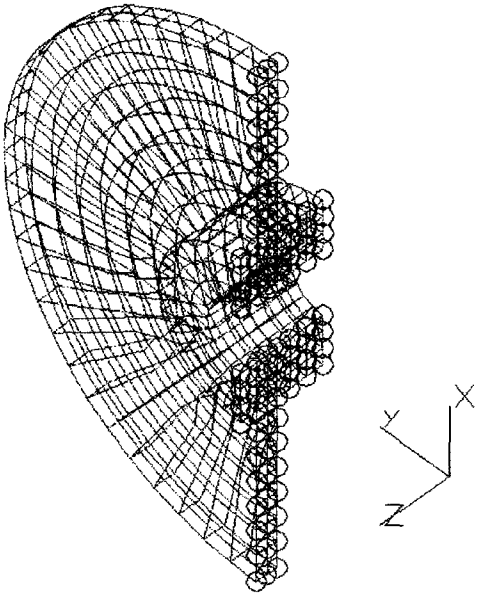

FIGURE 4.4 End plate and hub modeled with brick elements

location of nodes that are constrained with symmetry boundary conditions. There are no other boundary conditions on the nodes of this portion of the model, but it is of value to mention again that brick elements are already constrained in rotations about the x-, y-, and z-axis.

The outer shell and the stiffening rings of the roll body were modeled using the Type 6 plate/shell elements, shown in Figure 4.5. The circled nodes represent

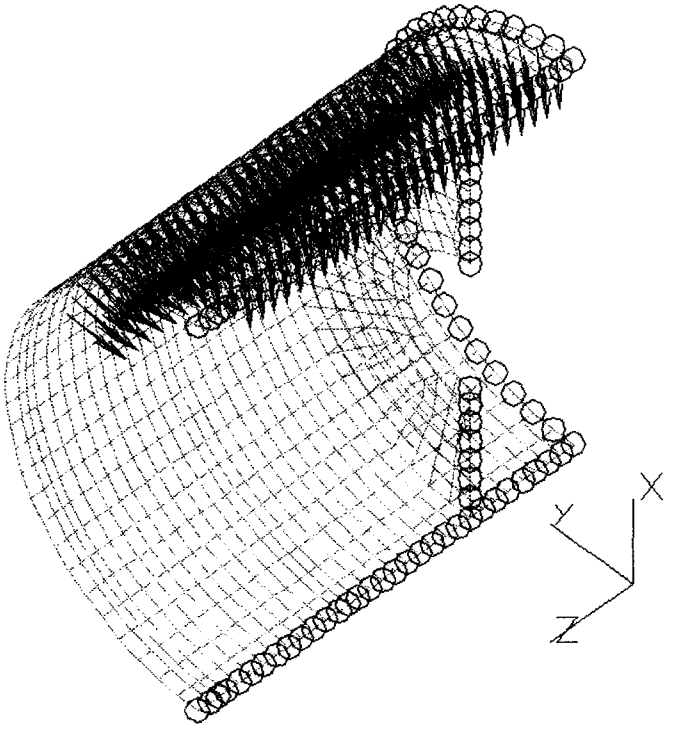

FIGURE 4.5 Roll body and stiffener modeled with plate elements

symmetry boundary condition just as in the other two element types. This portion of the model shows the pressure load that was used to approximate the force transmitted to the roll body from the sheet metal. The equivalent pressure was determined by taking the total force applied to the strip and dividing it by the effective surface area of contact. Figure 4.6 shows the technique used to derive an equivalent pressure of 15 psi. This ensures that the total applied force to the roll from the loaded strip metal is still equal to 24000 lbs. in the y-direction and 0 lbs. in the x-direction for the full roll. For the quarter model, the total applied

force is equal to 6000 lbs. in both the x and y-directions. This is not a problem, though, because the symmetry boundary conditions account for the net positive force value in the x-direction.

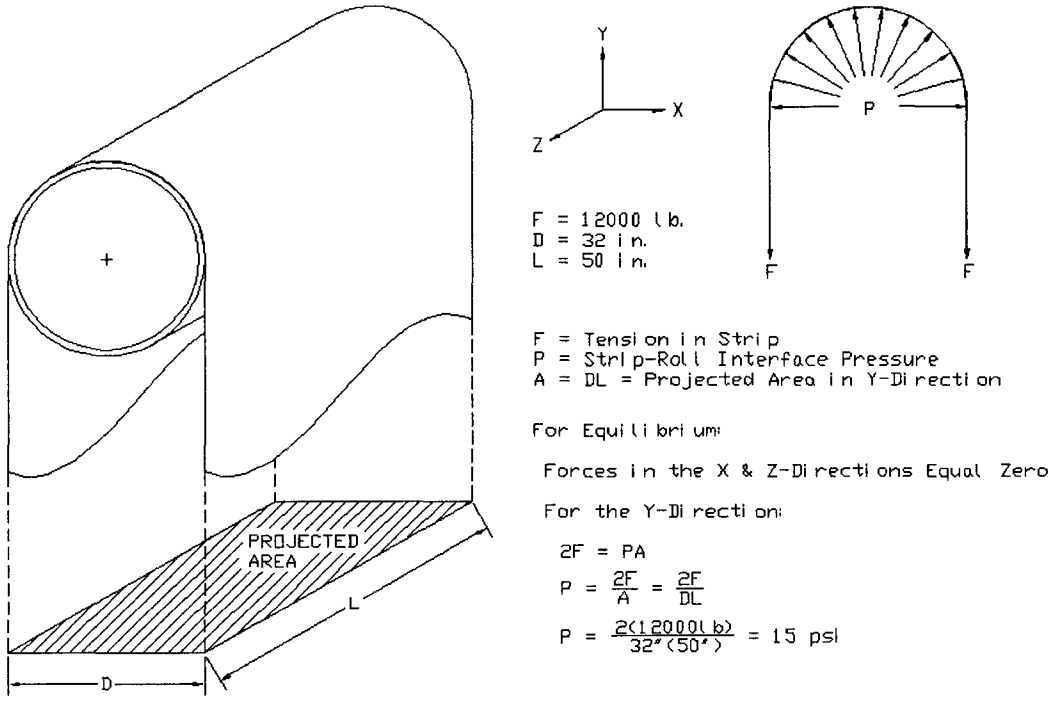

Figure 4.6 Determination of equivalent pressure

As can be seen in Figures 4.3 – 4.5, each of the element types were first drawn individually in the Superdraw II program of the software package. The material and area properties were input in the Bedit and Decoder programs, and then the sections were combined in the Combsst program. The roll shaft (beam elements) was first grafted/connected to the roll body shell and stiffening rings (plate elements). It should be noted that none of the nodes of these two element types are actually shared. The end plate and hub (brick elements) were then grafted to this assembly. The brick elements had nodes that were shared with both the

beam and the plate elements; thus tying the entire roll assembly together. Figure 4.7 shows the finite element model of an accumulator roll using ¼ symmetry.

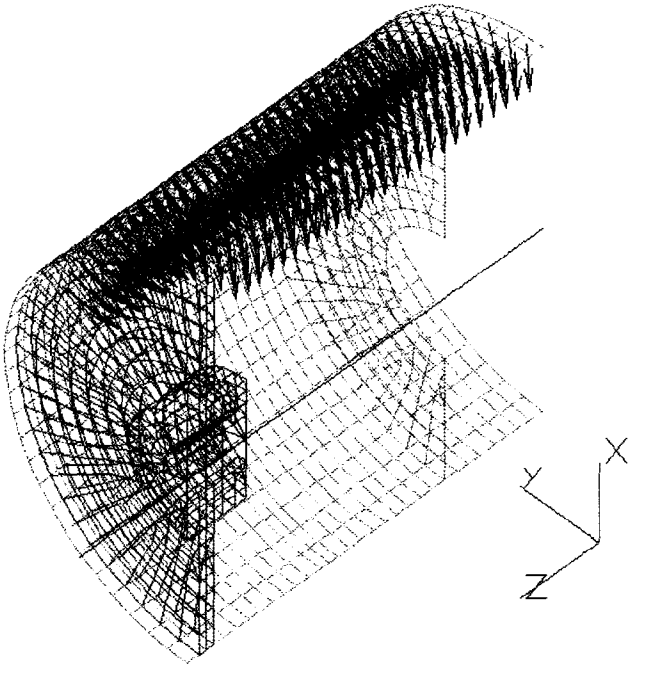

FIGURE 4.7 Complete finite element model of a one quarter accumulator roll

4.2 MODEL VARIATIONS

The finite element model illustrated in Figure 4.7 is of a standard accumulator roll with 2 stiffeners located 8.25" from the longitudinal line of symmetry. This is considered the first base model in this investigation. The dimensions of this roll are as stated in chapter 2. From this model, the first component of the roll design to be varied was the stiffener location. There is no set standard available as to the required number or placement of these disks within the roll body. Because these transverse disks must be welded to the inside of the body, they are very

labor-intensive additions to the roll. Consequently, it would be advantageous to the roll designer to know the effect each disk and its placement has on the displacements of the roll when it is loaded by the strip metal. Therefore the placement of the stiffeners was varied from 16.25" to 4" from the longitudinal line of symmetry then to one stiffener located at the line of symmetry and ultimately to no stiffener at all.

At this point, three base models were considered in the rest of the roll component variations: one with two stiffeners at 8.25" from the longitudinal line of symmetry shown previously in Figure 4.7, one with one stiffener at the longitudinal line of symmetry shown in Figure 4.8, and one with no stiffener shown in Figure 4.9.

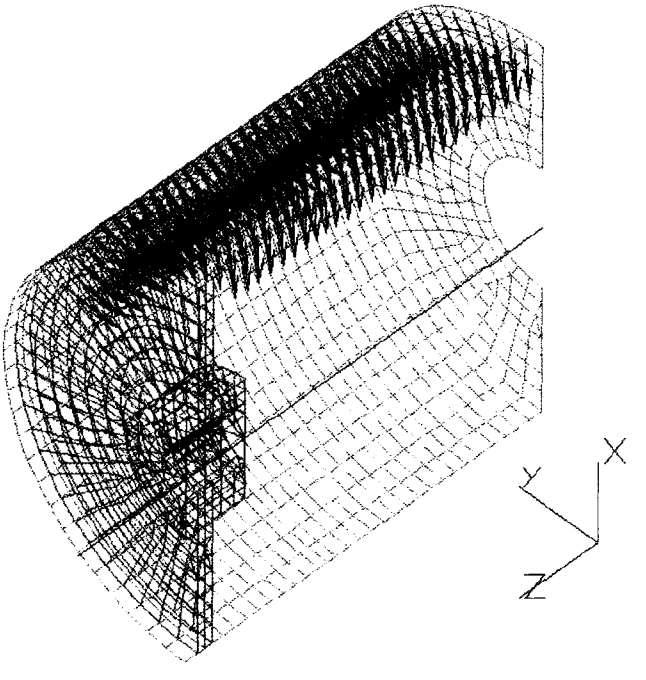

FIGURE 4.8 Complete finite element model with one stiffener at the longitudinal line of symmetry

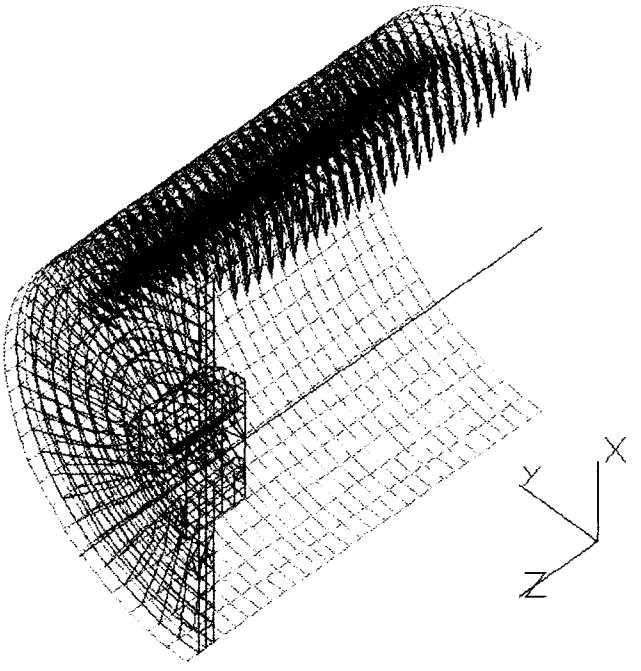

FIGURE 4.9 Complete finite element model with no stiffeners

It is of value to note again that Figure 4.7 only shows one of the two stiffeners because of the ¼ model symmetry. Also, Figure 4.8 shows one stiffener as well but the thickness is input in the program solver as ½ of the actual value because the stiffener is situated right at the line of symmetry.

From each of these base models, three roll component dimensions were varied. The stiffener thickness was varied from ¼" to 1", the roll body thickness was varied from ½ " to 2", and the end plate thickness was varied from 1" to 1⅝". A full list of the models considered and how the components of each varied from the original model can be found in Table A.1 of the appendix.

CHAPTER 5

RESULTS AND DISCUSSION

5.1 OVERVIEW

As each of the parameters of the original roll design were varied, suitable techniques to analyze the impact the changes had on the functioning of the roll had to be employed. One of the techniques used in this research was stress analysis of the end plate and the roll body. The total von Mises stress profiles from the finite element results of these areas were illustrated and the maximum von Mises stress was tabulated for comparison. Stress in the shaft was not presented as a comparative tool because, as stated previously, the shaft size is dictated by ASTM standards. Regardless, it was found that the stress in the shaft did not change with the parameter variations performed in this research. Also, the stress in the stiffeners was not presented because it was found to be insignificant and unchanging.

Another technique used for comparison of the various roll configurations was deflection of the end plate and the roll body. Deflections of each of these roll components were first compared illustratively by viewing the deflection profiles from the finite element results. This helped formulate a concept of the impact the

design changes had on the overall deflections in the roll. In addition, the maximum deflections in the end plate and the roll body were tabulated for comparison. Then, the deflections of the top line of nodes of the roll body were plotted on the same graph for the various roll configurations to further understand the impact of the design changes.

5.2 VARIATION OF STIFFENER LOCATION

As was stated previously, the first variation in roll design that was investigated was the placement of the stiffening disks within the roll body. Figures 5.1 shows the von Mises stress in the roll body as the stiffener location is varied from a position right at symmetry to a position 16.25" from symmetry to no stiffener at all. When viewing these pictures it is of value to note that the end plate is on the left side of the pictured rolls and therefore the line of symmetry is on the right side. Notice, the portion of the roll body that is between the end plate and the stiffener reacted to the applied pressure in a manner similar to a pin-pin beam. The portion of the roll body to the left of the stiffener reacted to the pressure in a manner similar to a cantilever beam. Therefore, the stress state of the portion of the roll body between the end plate and the stiffener reduced and the stress state of the portion between the stiffener and the line of symmetry increased as the stiffener was moved toward the end plate. The largest overall stress state was in the roll that has no stiffener at all because the roll body was subject to a cantilever type situation. The lowest and most uniform stress state occured when the stiffener was between 8.25" and 12.25" from the line of symmetry.

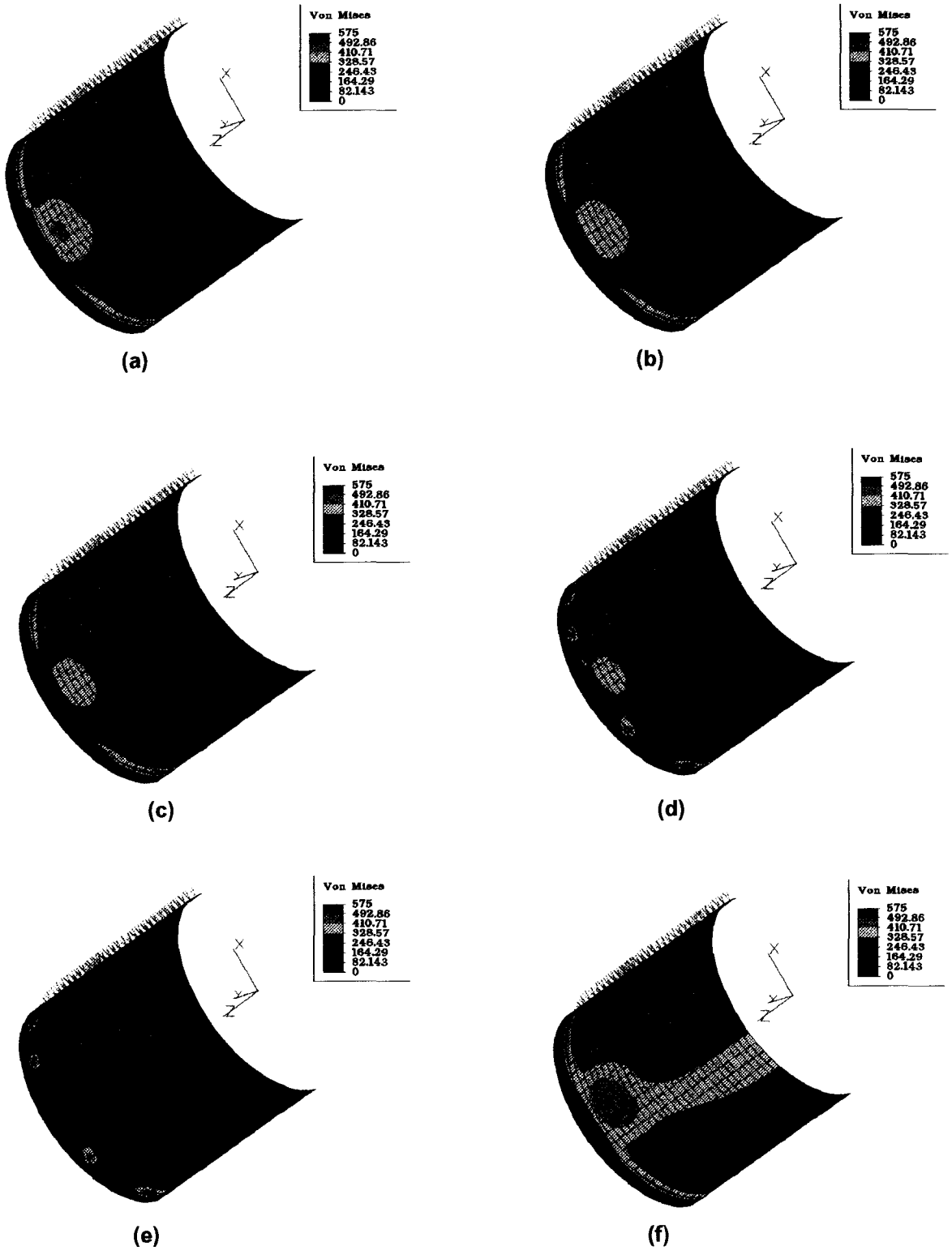

Figure 5.1 von Mises stress in roll body as stiffener is varied from **(a)** right at symmetry, **(b)** 4" from symmetry, **(c)** 8.25" from symmetry, **(d)** 12.25" from symmetry, **(e)** 16.25" from symmetry, **(f)** no stiffener

Although the placement of the stiffener had minimal effect on the maximum von Mises stress in the roll body, the stress distribution profile of the roll body showed significant sensitivity to stiffener placement. On the other hand, the placement of the stiffener had virtually no effect on both the maximum von Mises stress and the stress distribution profile in the end plate. Figure 5.2 shows the von Mises stress distribution of the end plate for all the variations in stiffener location.

Figure 5.2 von Mises stress distribution in endplate for all stiffener locations

The highest stress regions occurred at the end plate to hub interface at the top and bottom positions. It was expected, considering how the roll was loaded, that the maximum compressive stress would occur in the end plate at the top of the hub. Likewise, the maximum tensile stress would occur in the end plate at the bottom of the hub. This is because of the manner in which the end plate was situated within the roll. The shaft was rigidly connected to the hub and roll body. Therefore, when the roll body was pressure loaded the distortion in the end plate gave rise to the shown stress distribution. Because of the bulk size of the hub

compared to the roll body, the center of the end plate was more rigid and therefore saw higher stress.

The deflection profiles, shown in Figure 5.3, provided even more information into the analysis of stiffener location. Notice that the nearly vertical deflection contours in the roll body, as seen in the rolls with the stiffener at 8.25" and 12.25" from the line of symmetry, indicated minimal distortion and thus uniform deflection of this roll component. Therefore, in the rolls with the stiffener in this region of the roll, the roll body maintained its circular shape. On the other hand, in the rolls with the stiffener at the line of symmetry and 4" from the line of symmetry, the deflection contours jet to the right at the roll body top and bottom in-between the stiffener and end plate. This indicated more distortion in this portion of the roll body causing it to become slightly oval. As the stiffener got closer to the end plate, 16.25" from the line of symmetry, some of the deflection contours again jet to the right at the roll body top and bottom indicating roll body distortion. However, for this roll configuration, it was in the region to the right of the stiffener. The region of the roll body between the stiffener and the endplate maintained the vertical deflection contours. This is because the stiffener was close enough to the end plate to again ensure minimal distortion of that region of the roll body. When no stiffener was used, the deflection contours jet significantly to the right at the top and bottom of the roll body along the entire length of the roll. Without a stiffener there was no intermediate point within the roll to maintain the circular integrity.

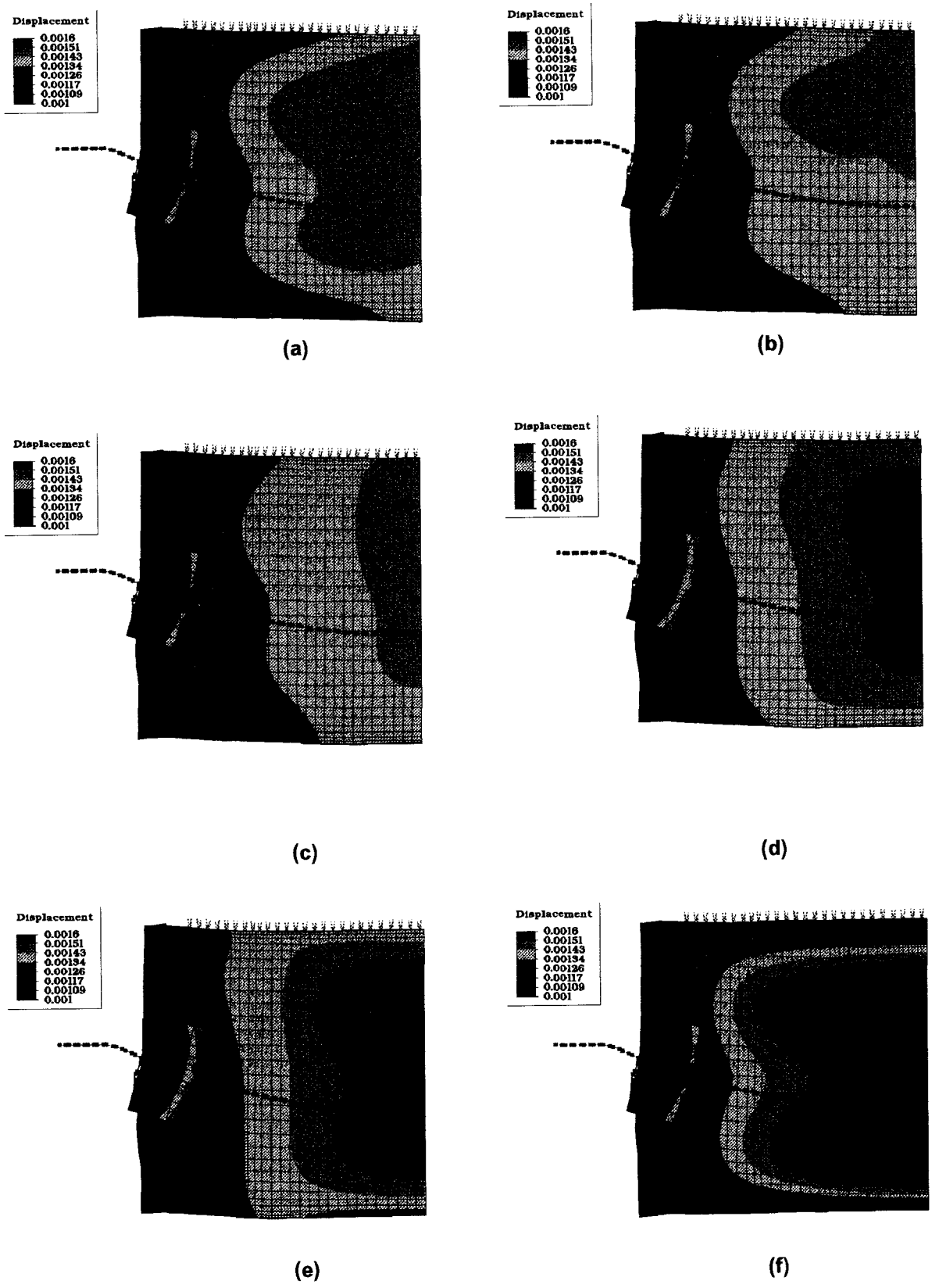

Figure 5.3 Deflection in roll as stiffener is varied from **(a)** right at symmetry, **(b)** 4" from symmetry **(c)** 8.25" from symmetry, **(d)** 12.25" from symmetry, **(e)** 16.25" from symmetry, **(f)** no stiffener

This distortion was slight in terms of absolute displacement and may very well be tolerable from a roll functioning view point. However, from a comparative view point, it was a significant deviation from the other roll configurations. This is illustrated in Figure 5.4 which shows the distortion of the roll body at the line of symmetry for the roll with the stiffener 8.25" from the line of symmetry and for the roll with no stiffener.

Figure 5.4 Distortion of roll body **(a)** with stiffener 8.25" from symmetry and **(b)** with no stiffener

As was seen in the stress profiles, the placement of the stiffener had practically no effect on both the maximum deflection and the deflection profile in the end plate. Therefore, the distortion of the endplate, shown in Figure 5.3, was practically identical for all the stiffener locations. Figure 5.5 shows another view of the deflection distribution and distortion of the endplate for all variations in stiffener location. The hub is also shown in the figure so that the distortion in the end plate at the end plate to hub interface can more readily be seen. The

maximum distortion occurred close to this interface at the top and bottom positions which was consistent with the highest stress region.

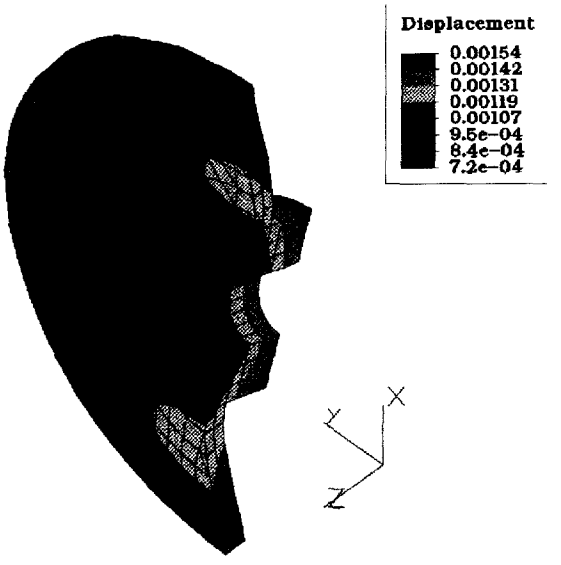

Figure 5.5 Displacement distribution in endplate for all stiffener location

The maximum deflection and von Mises stress for each of the rolls with variation in the stiffener location is tabulated in Table 5.1 below. This table includes intermediate stiffener locations that were not illustrated previously.

Table 5.1 Maximum deflection and von Mises stress as stiffener location is varied

	ROLL CONFIGURATION		MAXIMUM VON MISES		MAXIMUM DEFLECTION	
MODEL NAME	NUMBER OF STIFFENERS	STIFFENER LOCATION	END PLATE (psi)	ROLL BODY (psi)	END PLATE (in)	ROLL BODY (in)
ads6z	0	none	1418	511	1.17E-03	1.79E-03
ads5z	1	0	1418	548	1.17E-03	1.50E-03
ads7z6	1	4	1420	551	1.17E-03	1.45E-03
ads7z5	2	6.25	1420	555	1.17E-03	1.47E-03
ads3z	2	8.25	1421	566	1.17E-03	1.48E-03
ads7z1	2	10.25	1428	616	1.19E-03	1.53E-03
ads7z2	2	12.25	1434	673	1.23E-03	1.58E-03
ads7z3	2	14.25	1435	681	1.23E-03	1.61E-03
ads7z4	2	16.25	1437	689	1.23E-03	1.64E-03

Note that the maximum von Mises stress in the end plate occurred at the hub to end plate interface and the maximum von Mises stress in the roll body occurred at the end plate to roll body interface.

Lastly, in order to provide a graphical view of the deflection trend that occurred as the stiffener location was varied, the deflection of the top line of nodes is graphed for the various stiffener positions. Although this was not the site of maximum deflection, it proved useful in establishing a base line for deflection for each of the stiffener locations. Then the deflection of this set of nodes could be compared to the deflection of the same set of nodes as the stiffener location remained constant and other roll parameters were varied.

Due to the large number of stiffener locations, the deflections are presented on two graphs for clarity. Figure 5.6 shows the roll body deflection of the top line of nodes as the stiffener location was varied from a stiffener right at the line of symmetry to a stiffener that was 8.25" from the line of symmetry. Notice that the vertical deflection scale was inverted so that as the deflection of roll body increased, the graph goes down. Referring to this figure, it seems as though the roll with the stiffener at the line of symmetry had the least deflection. Indeed it did at the top line of nodes. However, all of the rolls had approximately the same overall downward vertical deflection. Therefore, it was the distortion of the roll body between the end plate and the stiffener that caused the top of the roll body to rise slightly when compared to the other roll bodies on this graph. In fact any

change in the slope on the graph of the top line of nodes of the roll body indicated distortion of the roll body from circular to oval. Therefore, the graph indicated that the best position of stiffener for roll body integrity was 6.25" from the line of symmetry.

Figure 5.7 shows the roll body deflection of the top line of nodes as the stiffener location was varied from 8.25" from the line of symmetry to 16.25" from the line of symmetry to no stiffener at all. Following the same logic explained for the previous graph, the distortion of the roll body of this set of stiffener locations occurred to the right of the stiffener in the area between the stiffener and the line of symmetry. Also, since the graph of the roll with no stiffener actually rose, it indicated again the marked distortion of the roll body compared to the other roll configurations.

At this point in the analysis, three base models were chosen from the variety of stiffener locations in order to concisely analyze the impact changes in certain roll parameter thicknesses had on the stresses in and the deflections of the roll. Although the roll with two stiffeners located 6.25" from the longitudinal line of symmetry was better in terms of both the roll body integrity and the maximum von Mises stress when compared to the roll with stiffeners located 8.25" from symmetry, the latter was chosen for further analysis. This is because these two were actually very similar in all respects and the 8.25" was the dimension supplied by a roll manufacturer.

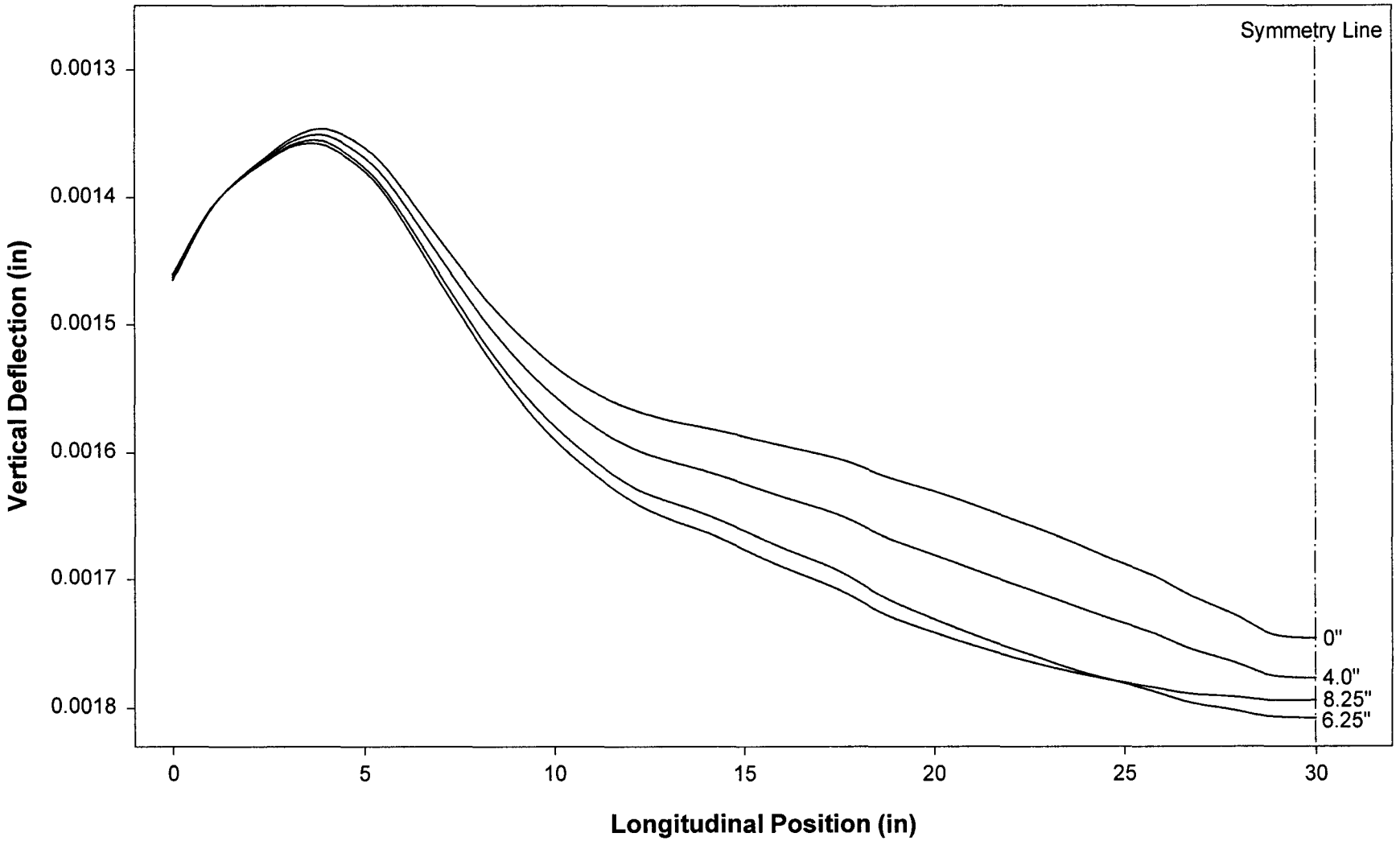

Figure 5.6 Roll body deflection with variation in stiffener location from 8.25" to 0"

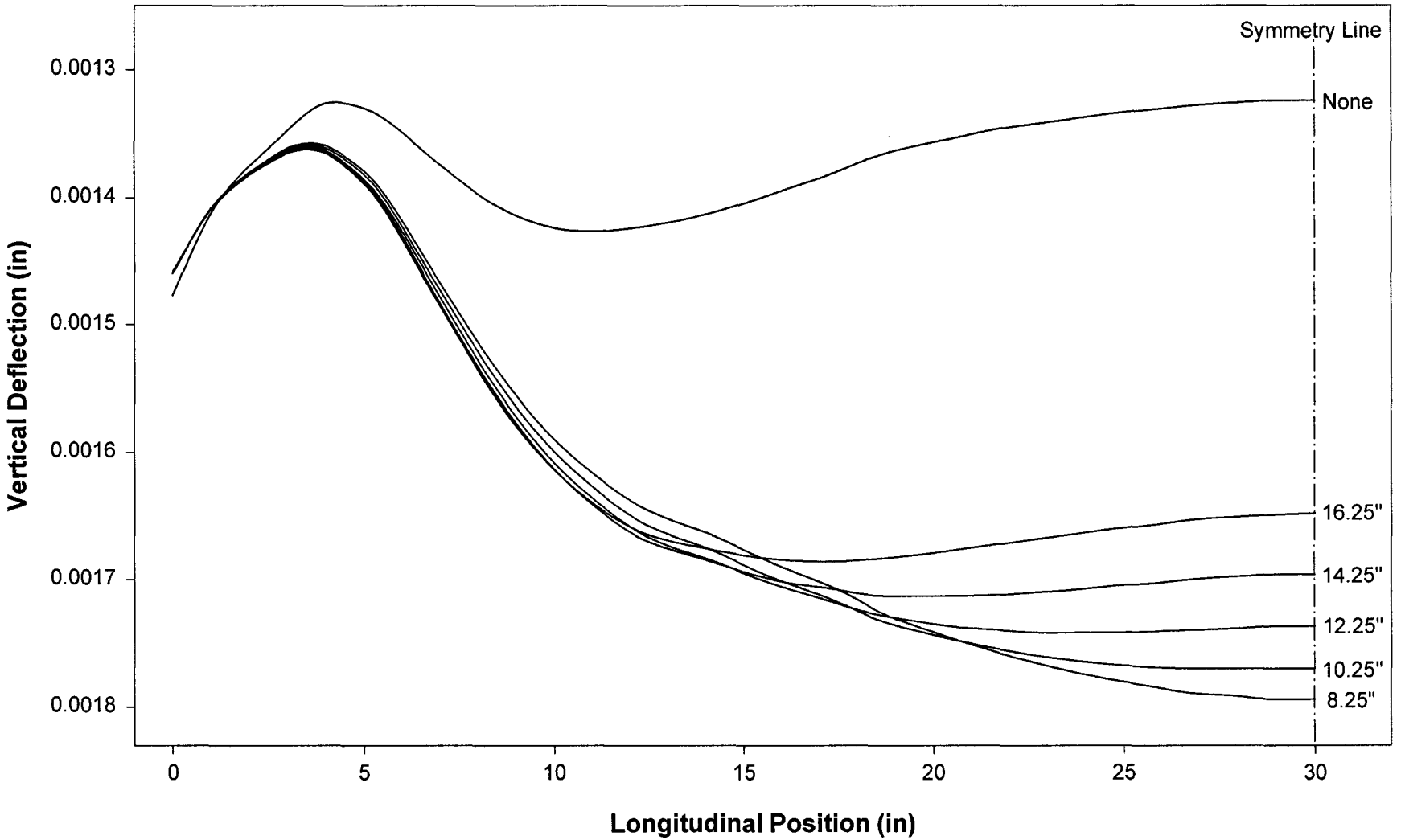

Figure 5.7 Roll body deflection with variation in stiffener location from 8.25" to 16.25" to no stiffener

The second base model chosen for further analysis was the roll with one stiffener located right at the line of symmetry. This was chosen because although there was some distortion in the roll body, it may have proved to be minute enough to be a viable roll configuration. The elimination of one stiffener would certainly be desirable from a roll manufacturing stand point.

The final base model chosen was the roll with no stiffener at all. Although this roll configuration seems an unlikely candidate given the distortion shown in the roll body, it was chosen to see if changing other parameters of the roll might alleviate some of the distortion thus making it a viable option. Also, since tolerable absolute and relative deflections of the roll and roll body were not fully known, it was reasoned that information concerning this configuration could prove useful when that information became available.

The deflections of the top line of nodes of these three base models are presented together for summary in Figure 5.8. From this point, the base models will be referred to as the roll with two stiffeners, one stiffener, or no stiffeners. The graph provides the basic characteristic deflection profiles of the top line of nodes for each base model to which other roll configurations will be compared.

As stated previously, the roll parameters that were varied next for each base model included the stiffener thickness (for the one and two stiffener rolls), the roll body thickness and the end plate thickness.

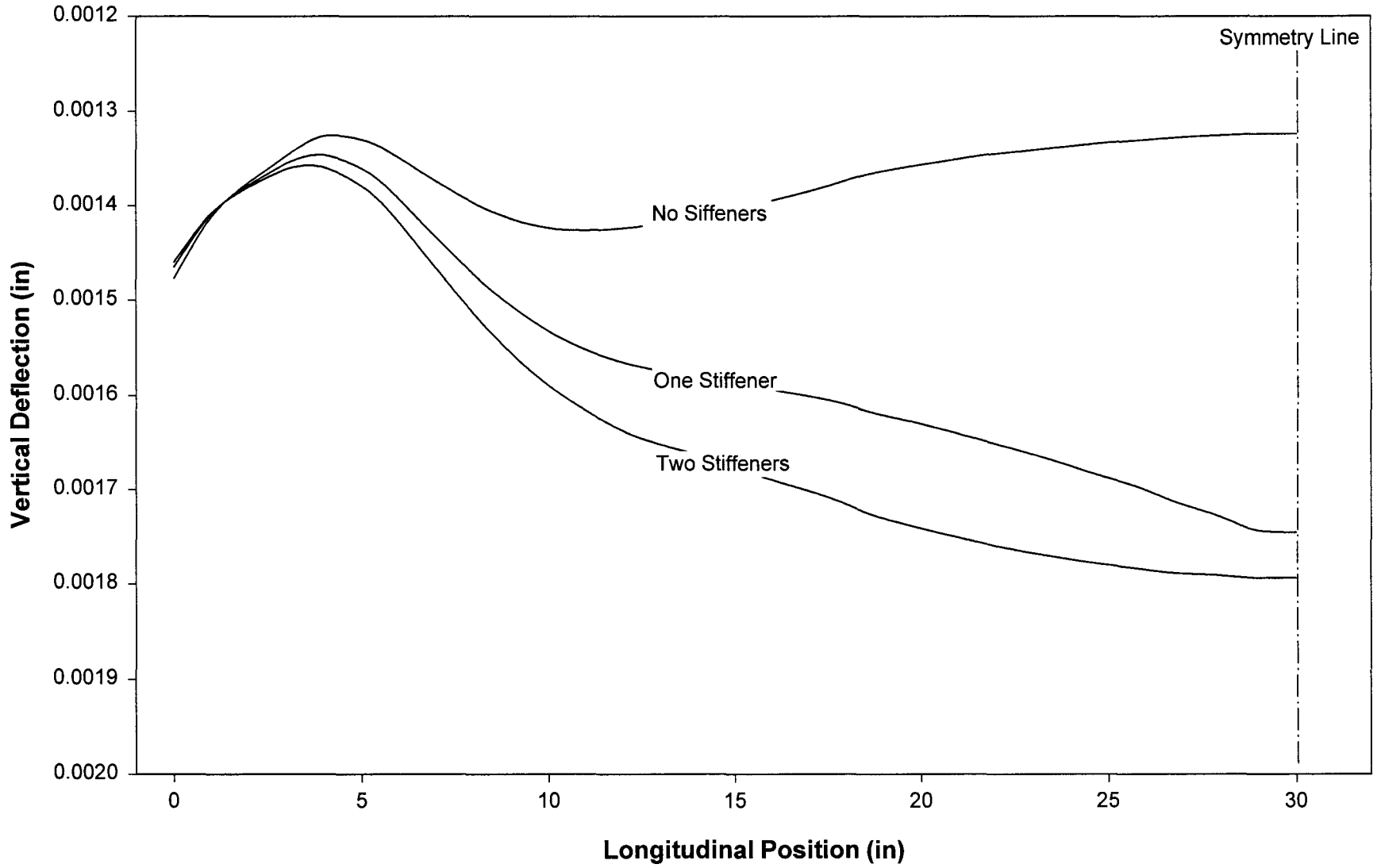

Figure 5.8 Roll body deflection profiles of base models

5.3 VARIATION OF STIFFENER THICKNESS

The next variation in the roll design that was investigated was the thickness of the stiffening disks within the roll body. It was desirable to determine the impact that this variation had on the functioning of the roll for two reasons. In the roll with two stiffeners, a thinner stiffener would save material costs and lighten the weight of the roll. In the roll with one stiffener, a thicker stiffener might lessen some of the roll body distortion thereby allowing the one stiffener to be a more acceptable choice. The material costs would still be lowered and the weight lightened. In addition, manufacturing costs would be lowered.

It was found that the change in stiffener thickness from ¼" to 1" caused no change in any of the analysis techniques employed in this research. This can be seen in Table 5.1 in which the maximum deflection and the maximum von Mises stress for each stiffener thickness variation is tabulated. There was no meaningful change in any deflection or stress value of any roll component.

Table 5.2 Maximum deflection and von Mises stress as stiffener thickness is varied

MODEL NAME	ROLL CONFIGURATION		MAXIMUM VON MISES		MAXIMUM DEFLECTION	
	NUMBER OF STIFFENERS	STIFFENER THICKNESS	END PLATE (psi)	ROLL BODY (psi)	END PLATE (in)	ROLL BODY (in)
ads8z1	2	0.25	1421	565	1.17E-03	1.49E-03
ads3z	2	0.5	1421	566	1.17E-03	1.48E-03
ads8z	2	0.75	1421	567	1.17E-03	1.48E-03
ads10z	2	1	1421	568	1.17E-03	1.48E-03
ads9z1	1	0.25	1418	547	1.17E-03	1.50E-03
ads5z	1	0.5	1418	548	1.17E-03	1.50E-03
ads9z	1	0.75	1418	549	1.17E-03	1.49E-03
ads11z	1	1	1419	550	1.17E-03	1.48E-03

The finite element stress and deflection profiles in the endplate and the roll body for the one stiffener and two stiffener rolls with variation in stiffener thickness were practically identical to the previous rolls with the stiffener at the line of symmetry and the stiffener 8.25" from symmetry, respectively. This was true for all the variations in stiffener thickness. Therefore, it is left to the reader to refer back to the appropriate figures if that information is desired.

The deflection graphs of the top line of nodes of the roll body for each variation in stiffener thickness showed the same result. Figure 5.9 shows the roll body deflection for the roll with two stiffeners. As the stiffener thickness was thinned, there was a very slight change in the leveling off of the nodes close to the line of symmetry. This indicated that the thicker stiffener prevented even less of the miniscule distortion found in the two stiffener roll. That change in deflection, however, was only 1.11% of the overall deflection when the stiffener thickness changed from ¼" to 1". This information indicated that a stiffener thickness of ¼" is a viable option providing the original roll was suitable for the application.

Figure 5.10 shows the roll body deflection for the roll with one stiffener. As with the two stiffener roll, as the stiffener was thinned from 1" to ¼", the distortion in the roll body was slightly improved. Again, however, the improvement in deflection over the entire stiffener thickness range from 1" to ¼" was a negligible amount, only 1.59%. Therefore, using a thicker stiffener in the one stiffener roll added no measurable advantage.

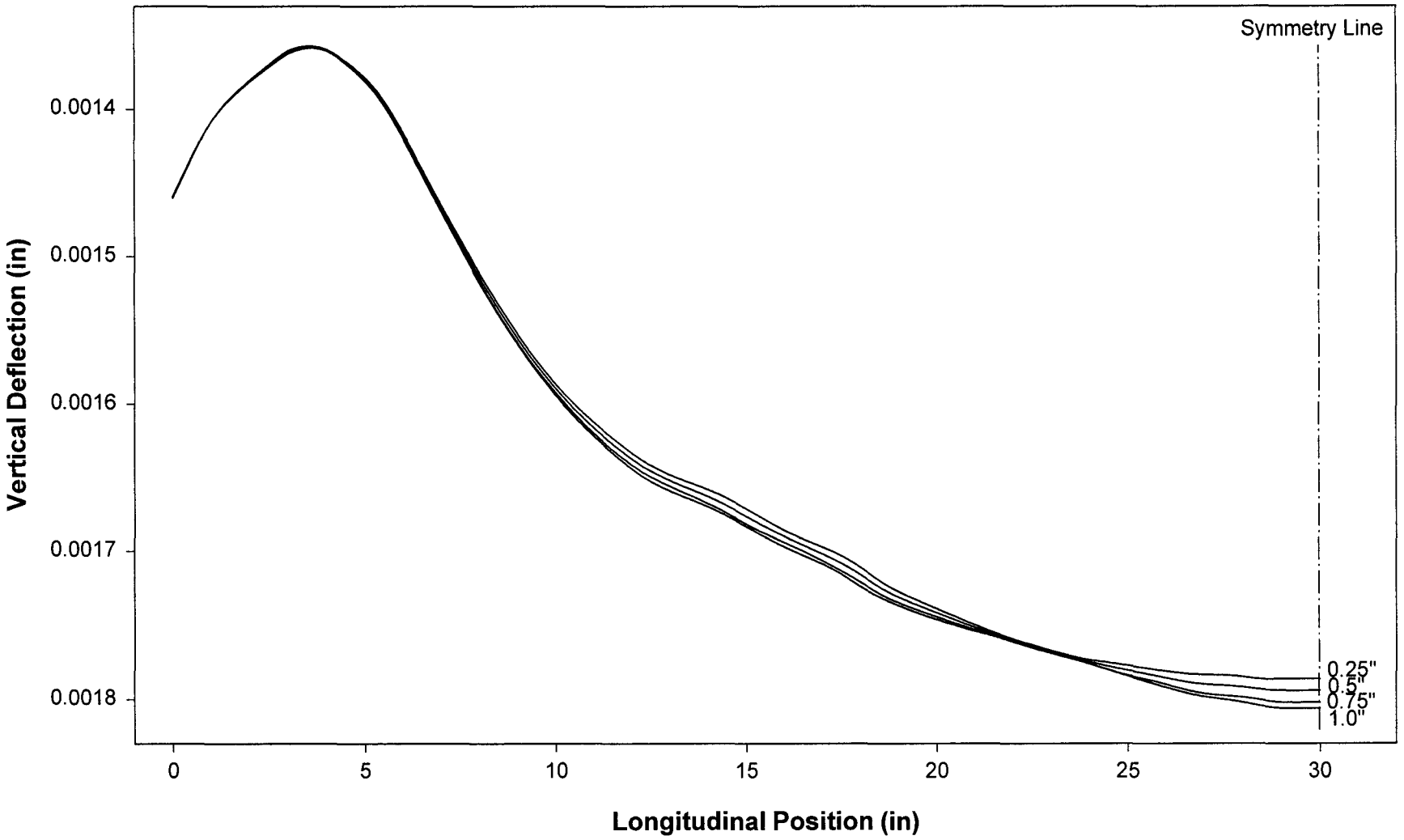

Figure 5.9 Roll body deflection with variation in stiffener thickness (two stiffeners)

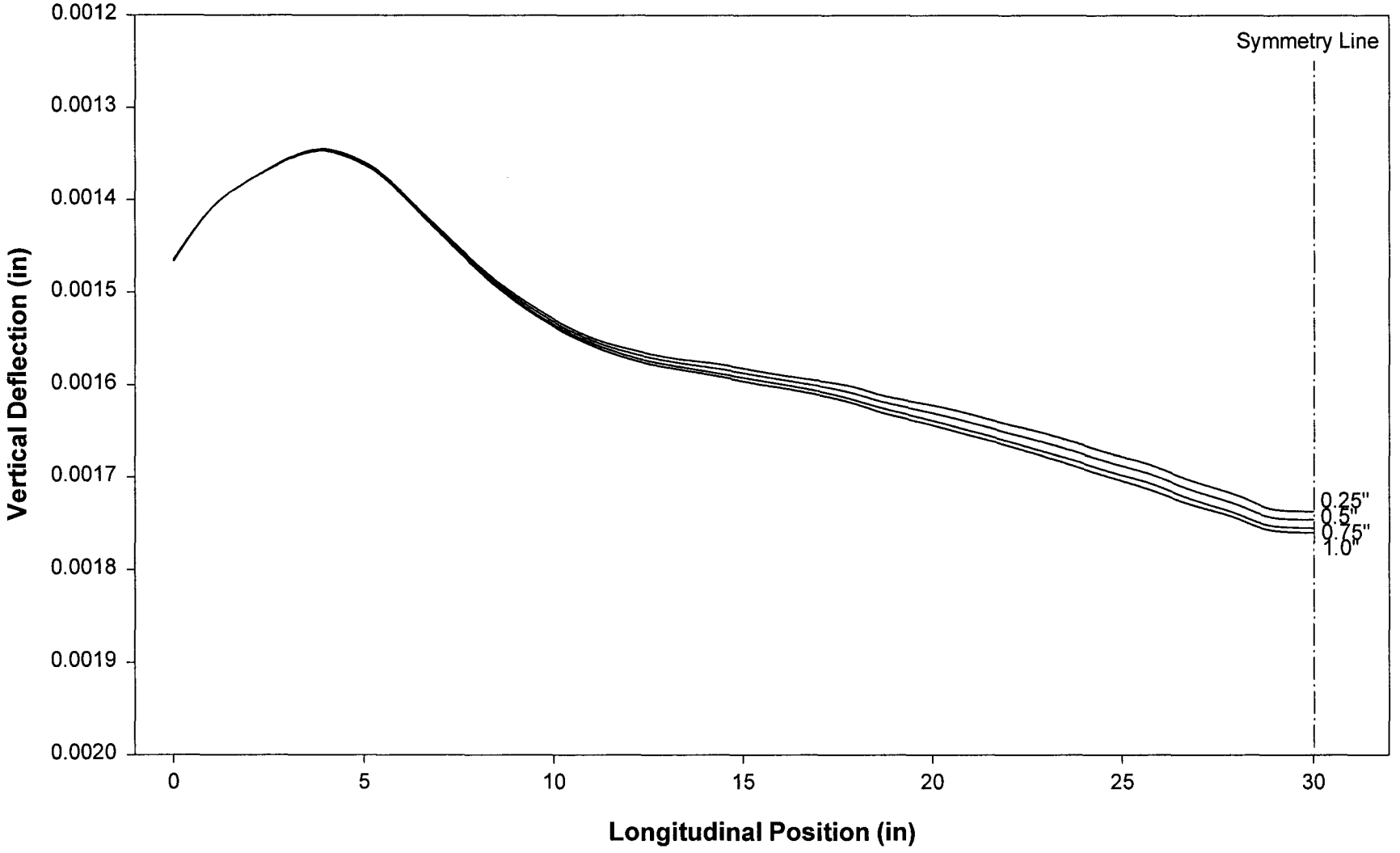

Figure 5.10 Roll body deflection with variation in stiffener thickness (one stiffener)

5.4 VARIATION OF ROLL BODY THICKNESS

The third variation in roll design that was investigated in this research was the thickness of the roll body. Figure 5.11 shows the von Mises stress in the roll body as the thickness was varied from ½" to 2" for the two stiffener roll.

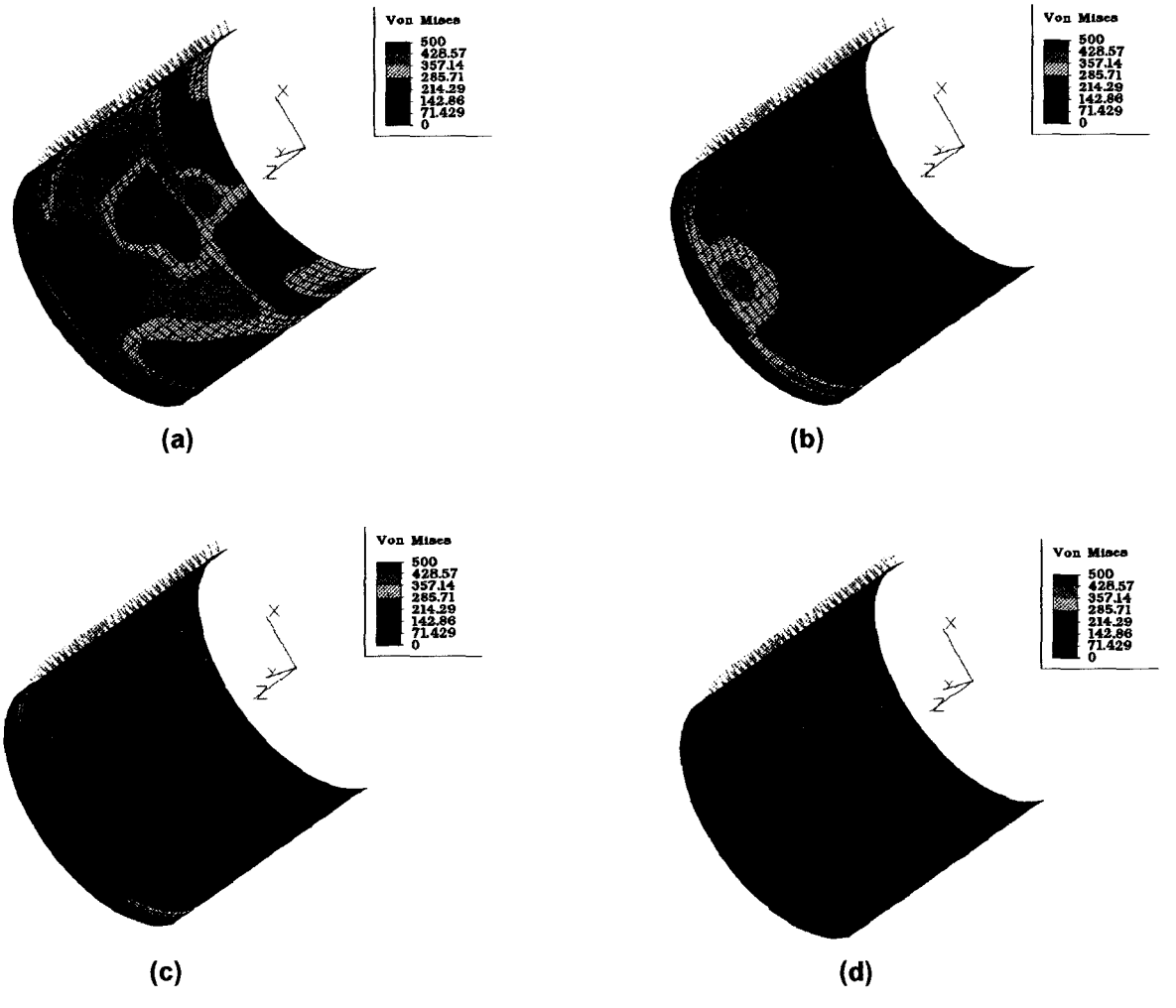

Figure 5.11 von Mises stress in the roll body of the two stiffener roll for roll body thickness of **(a)** 0.5", **(b)** 1.0", **(c)** 1.5", and **(d)** 2.0"

Notice that the scale range is slightly different from before to accommodate the relatively large range of von Mises stress. Although it may not be readily

apparent, the stress distribution profiles in the figure are actually quite similar. However, there was a significant difference in the absolute values of the stress. In fact, there was a 360% increase of the stress values in the roll body when the thickness was decreased from 2" to ½".

Likewise, the stress profiles of the end plate remained the same as the roll body thickness was varied and can be considered the same as the profile show in Figure 5.2. However, in contrast to the roll body stress values, there was a *decrease* in the end plate stress values as the roll body thickness decreased from 2" to ½". The decrease, though, was only 2.7% and is therefore viewed as insignificant.

The roll deflection profiles showed similar trends. Figure 5.12 shows the deflection of the roll as the thickness was varied from ½" to 2" for the two stiffener roll. Again notice that the scale range is different to accommodate the relatively large range of deflection values. Similar to the stress values in the roll body, the roll body deflection values increased as the roll body thickness decreased. In fact there was a 62% increase in deflection as the thickness decreased from 2" to ½". The deflection profiles of the roll bodies in the figure were also very similar to each other just as with the roll body stress profiles, except for the roll with thickness of ½". In this roll, the roll body not only deflected but also distorted. The maximum distortion occurred in two places: between the end plate and the stiffener and at the line of symmetry.

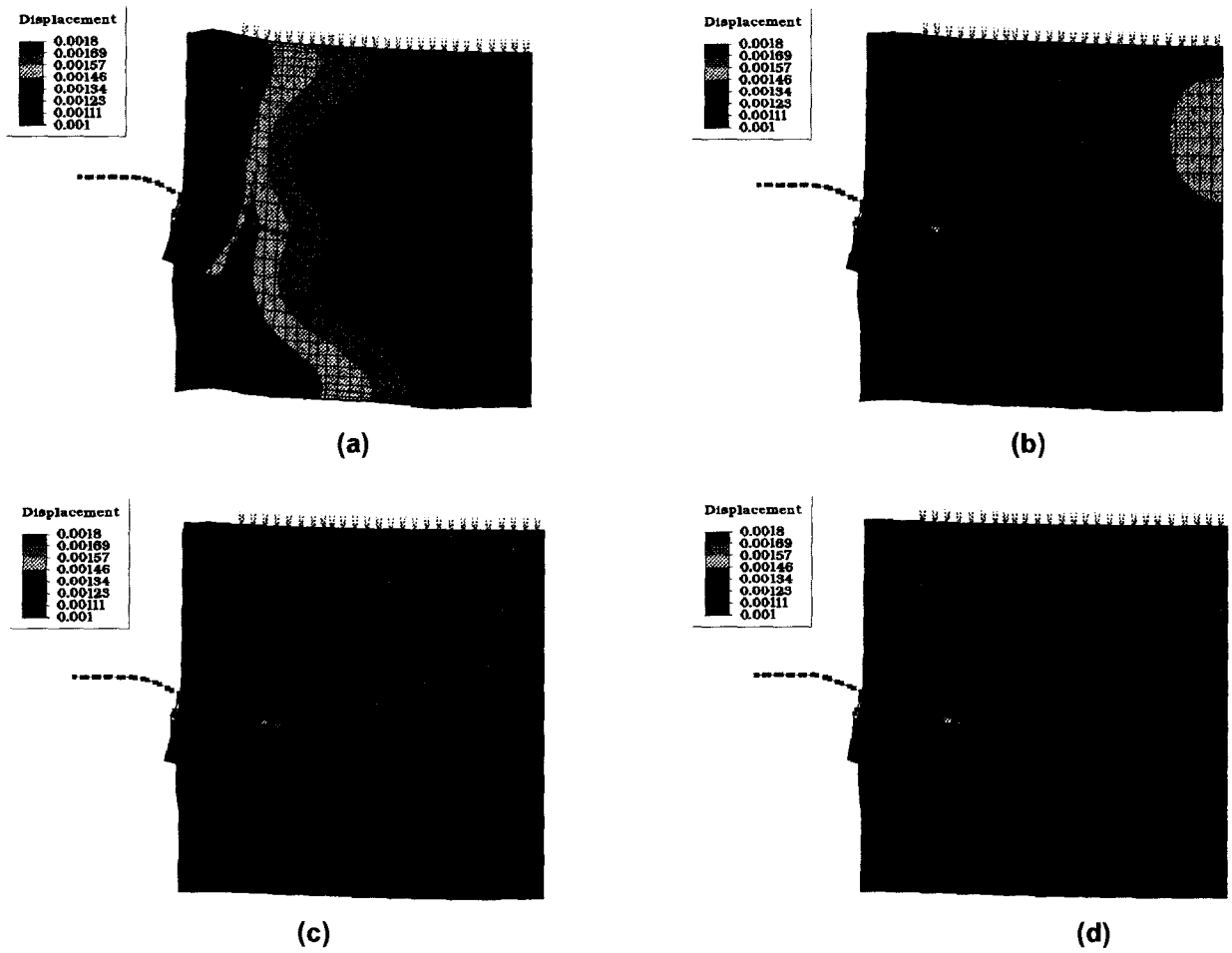

Figure 5.12 Deflection of the two stiffener roll as the thickness is varied from (a) 0.5", (b) 1.0", (c) 1.5", and (d) 2.0"

The distortion of the roll body at the line of symmetry is shown in Figure 5.13.

Figure 5.13 Distortion of two stiffener roll for roll body thickness **(a)** = 1.0" and **(b)** = ½"

Notice that the distortion is similar to the distortion shown in Figure 5.4(b) of the roll body that was 1" thick but with no stiffeners.

Unlike the stress in the end plate, the deflection in the end plate increased as the roll body thickness decreased. The increase in deflection was 16.2% as the roll body thickness decreased from 2" to ½". The deflection profiles remained the same, however, and are basically the same as was shown in Figure 5.5.

The one stiffener roll and the no stiffener roll showed similar trends in stress and deflection analyses presented for the two stiffener roll. One further interesting information to note, though, was the effect that the change in the roll body thickness had on the distortion in the body of the roll with no stiffeners. Figure 5.14 shows the distortion in the no stiffener roll for roll body thicknesses of ½" and 1½".

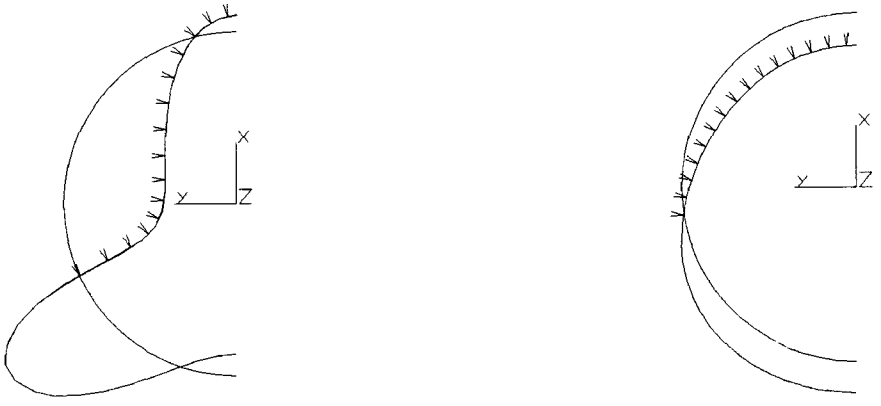

(a) **(b)**

Figure 5.14 Distortion of no stiffener roll for roll body thickness **(a)** = ½" and **(b)** = 1½"

The scale used in the above figure is the same as was used previously. Therefore, from a comparative view point, the distortion in the roll body changed significantly when the roll body thickness varied from ½" to 1½". At a thickness of 1½" or greater the roll body maintained its circular integrity.

Table 5.3 summarizes the maximum deflection and stress for all the roll configurations considered in this portion of the roll design investigation. Although the trends for the two, one, and no stiffener rolls are similar, the change in the roll

Table 5.3 Maximum deflection and von Mises stress as roll body thickness is varied

MODEL NAME	ROLL CONFIGURATION		MAXIMUM VON MISES		MAXIMUM DEFLECTION	
	NUMBER OF STIFFENERS	ROLL BODY THICKNESS	END PLATE (psi)	ROLL BODY (psi)	END PLATE (in)	ROLL BODY (in)
ads27z	2	0.5	1405	990	1.29E-03	1.99E-03
ads24z	2	0.75	1413	778	1.23E-03	1.74E-03
ads3z	2	1	1421	566	1.17E-03	1.48E-03
ads12z	2	1.125	1425	486	1.15E-03	1.42E-03
ads15z	2	1.25	1429	406	1.13E-03	1.37E-03
ads30z	2	1.5	1433	328	1.12E-03	1.31E-03
ads33z	2	1.75	1438	272	1.12E-03	1.27E-03
ads36z	2	2	1444	215	1.11E-03	1.23E-03
ads28z	1	0.5	1409	1004	1.29E-03	2.12E-03
ads25z	1	0.75	1414	776	1.23E-03	1.81E-03
ads5z	1	1	1418	548	1.17E-03	1.50E-03
ads13z	1	1.125	1422	473	1.15E-03	1.44E-03
ads16z	1	1.25	1427	398	1.13E-03	1.37E-03
ads31z	1	1.5	1432	322	1.12E-03	1.31E-03
ads34z	1	1.75	1437	267	1.12E-03	1.27E-03
ads37z	1	2	1442	212	1.11E-03	1.23E-03
ads29z	0	0.5	1446	1321	1.29E-03	4.29E-03
ads26z	0	0.75	1420	916	1.23E-03	3.04E-03
ads6z	0	1	1418	511	1.17E-03	1.79E-03
ads14z	0	1.125	1422	446	1.15E-03	1.65E-03
ads17z	0	1.25	1427	381	1.13E-03	1.50E-03
ads32z	0	1.5	1430	316	1.12E-03	1.36E-03
ads35z	0	1.75	1436	263	1.12E-03	1.31E-03
ads38z	0	2	1442	210	1.11E-03	1.26E-03

body thickness had a greater impact on the stresses in and the deflections of the roll body with no stiffener than for those of the two and one stiffener rolls. This is because the roll body geometrical stiffness for the no stiffener roll was obtained only from the stiffness of the roll body itself. The roll bodies of the two and one stiffener rolls gain geometrical stiffness from the stiffeners even before the added stiffness from an increase in thickness.

For the one stiffener roll, the von Mises stress in the roll body increased 373% and the deflection of the roll body increased 72% as the thickness decreased from 2" to ½". This is very similar to the increases presented for the two stiffener roll. For the roll with no stiffeners, however, the von Mises stress in the roll body increased as much as 529% and the deflection of the roll body increased 240% as the thickness decreased from 2" to ½".

Figures 5.15 to 5.17 show the trend in the deflection of the top line of nodes of the roll body for all the variations in roll body thickness. It is important at this point to again emphasize that the top line of nodes is not the position of maximum stress. So that while these graphs show the trend in the deflection of the roll body at any location along the roll circumference, they do not indicate the percent change in deflection at any circumferencial location *except* along the top. For example, the maximum deflection in the roll body of the one stiffener roll showed a 72% increase in deflection as the thickness decreased from 2" to ½". The graph in Figure 5.15 only shows a deflection increase of, at most, 34%.

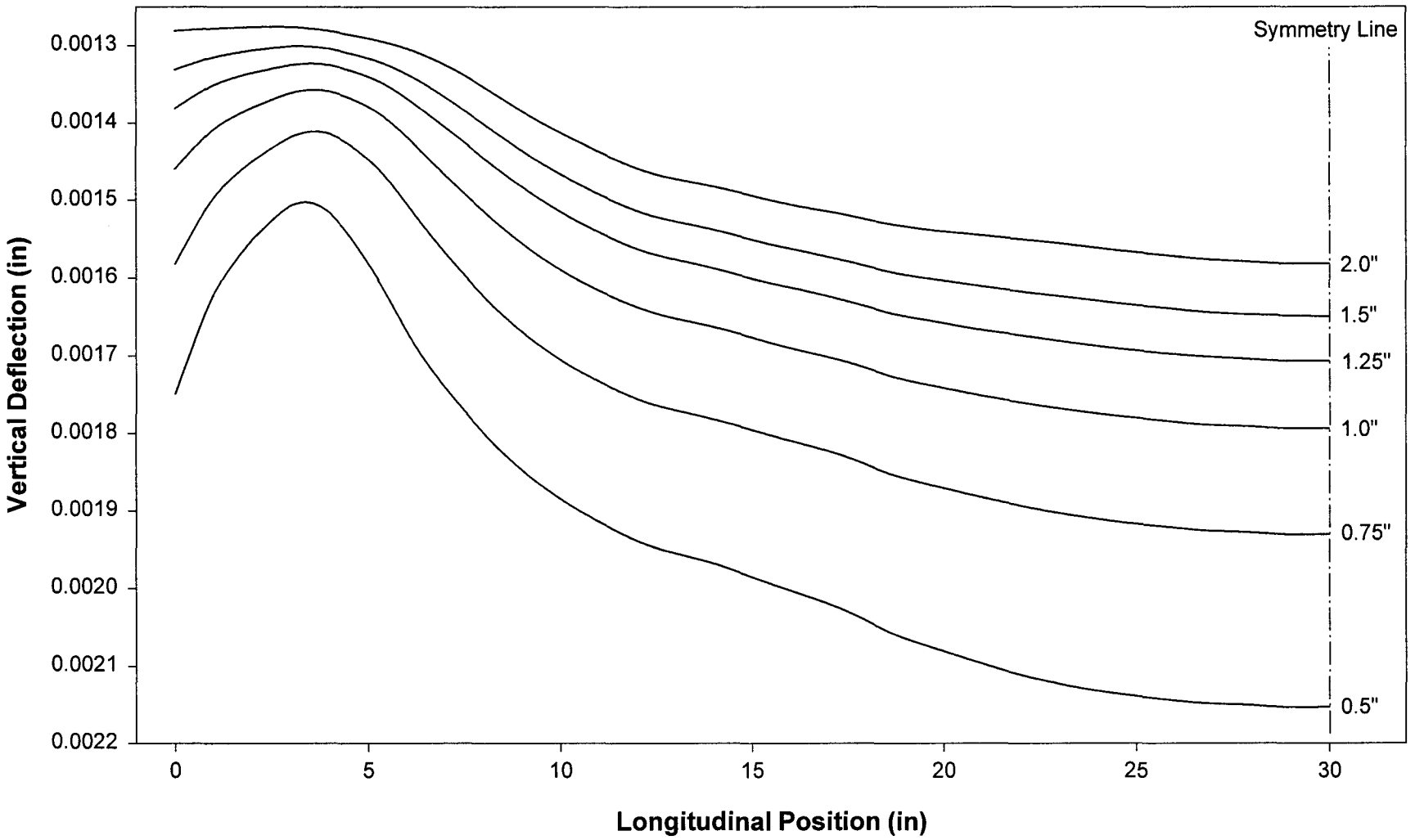

Figure 5.15 Roll body deflection with variation in roll body thickness (two stiffeners)

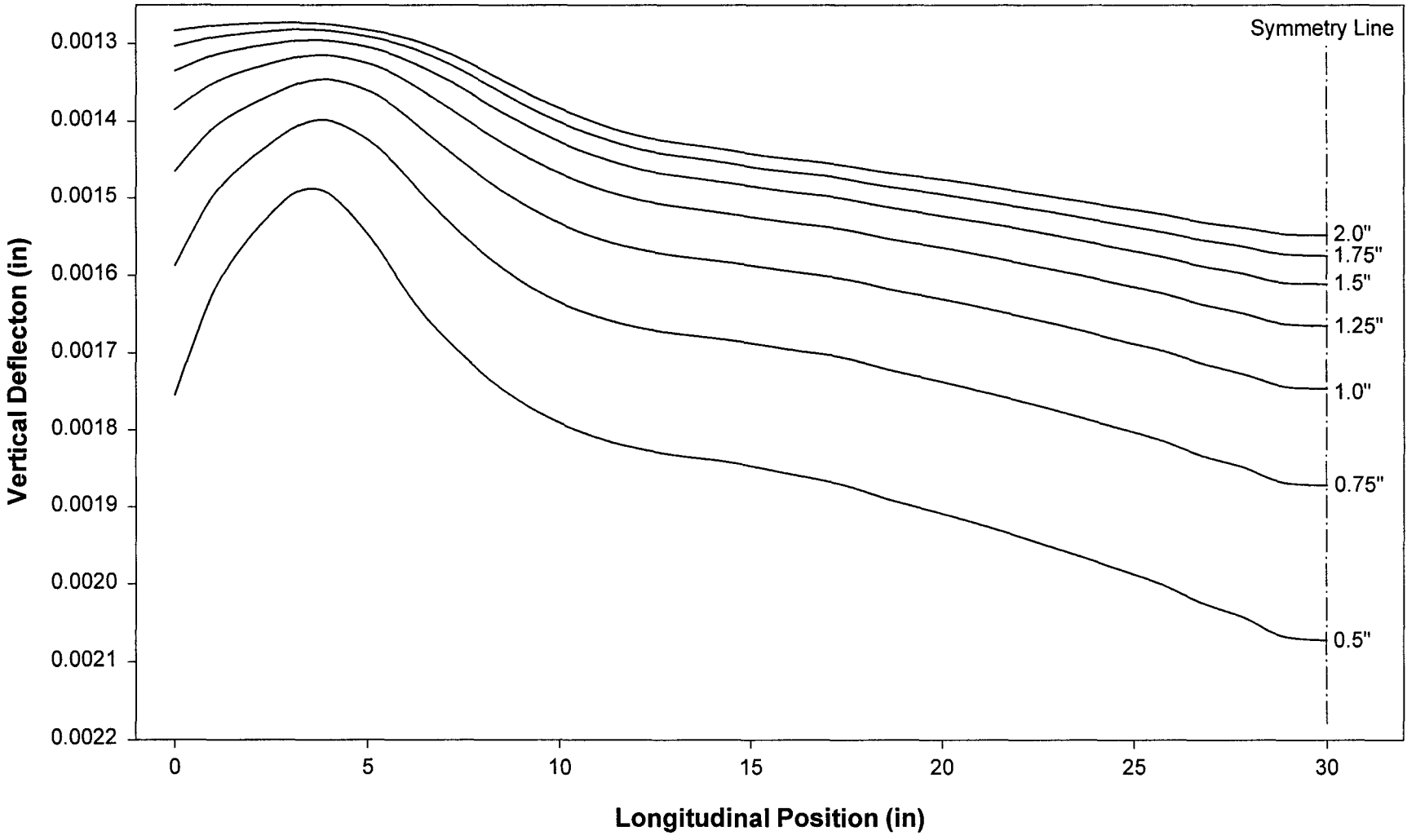

Figure 5.16 Roll body deflection with variation in roll body thickness (one stiffener)

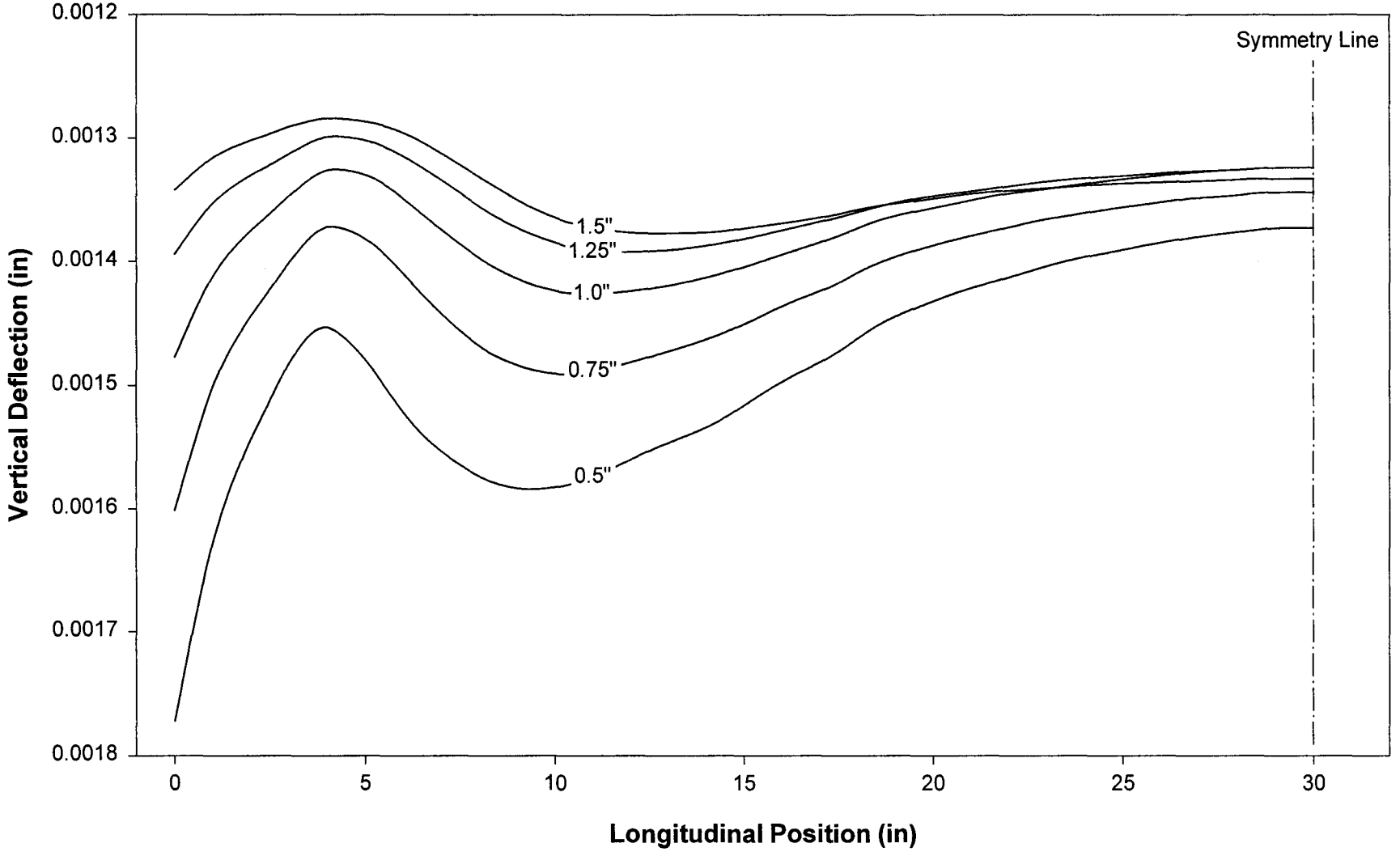

Figure 5.17 Roll body deflection with variation in roll body thickness (no stiffeners)

5.5 VARIATION OF END PLATE THICKNESS

The final variation in roll design that was considered in this research was the thickness of the end plate. The end plate was varied in thickness from 1" to 1⅝". Again, as with the other variations, knowing the effect changing the thickness of the end plate has on the functioning of the roll could lead to material and labor cost savings.

Varying the end plate thickness had minimal effect on the stresses in the roll body. The roll body stress had an increase in maximum von Mises stress of approximately 11% for the one and two stiffener rolls and a 5% increase in the maximum von Mises stress for the no stiffener roll. This increase, however, did not occur as the end plate thickness decreased from 1⅝" to 1". On the contrary, the roll body stress increased as the end plate thickness decreased from 1⅝" to 1¼" but then the roll body stress began to decrease as the end plate thickness continued to decrease from 1¼" to 1". This trend in maximum von Mises stress of the roll body was the same for all three base models. It is interesting to note that the maximum von Mises stress occurred in the rolls with the original value for the end plate thickness.

The deflection of the roll body, however, did not show this same pyramid of values as the end plate thickness decreased. Instead, there was again a steady increase in roll body deflection as the end plate thickness decreased from 1⅝" to

1". The one and two stiffener rolls had a roll body deflection increase of 22.6% and the no stiffener roll had a roll body deflection increase of 18.3%.

The largest effect the change in the end plate thickness had on the roll was the stresses in the end plate itself. The stress and deflection profiles for the one stiffener roll will be illustrated in this section and then extrapolations to the two stiffener and no stiffener rolls will be made just as was done in the previous section using the two stiffener roll. Figure 5.18 shows the end plate von Mises stress profiles in the one stiffener roll as the end plate thickness is varied from 1" to 1⅝". Notice in the figure that the scales for the von Mises stress profiles are different for each of the variations in end plate thickness. This is so that the similarities in the von Mises stress distribution profiles could easily be seen. Therefore, the significant change that occurred in the end plate as the thickness was varied was the absolute maximum von Mises stress value. This was the same occurrence that was noted for the maximum von Mises stress in the roll body as the roll body thickness was varied.

The increase in the maximum von Mises stress was approximately 70% as the end plate thickness decreased from 1⅝" to 1". Remember that in section 5.2, the location or absence of the stiffener was found to have no effect on the end plate stress values or stress profiles. Therefore, data for the two and no stiffener rolls were practically identical to this.

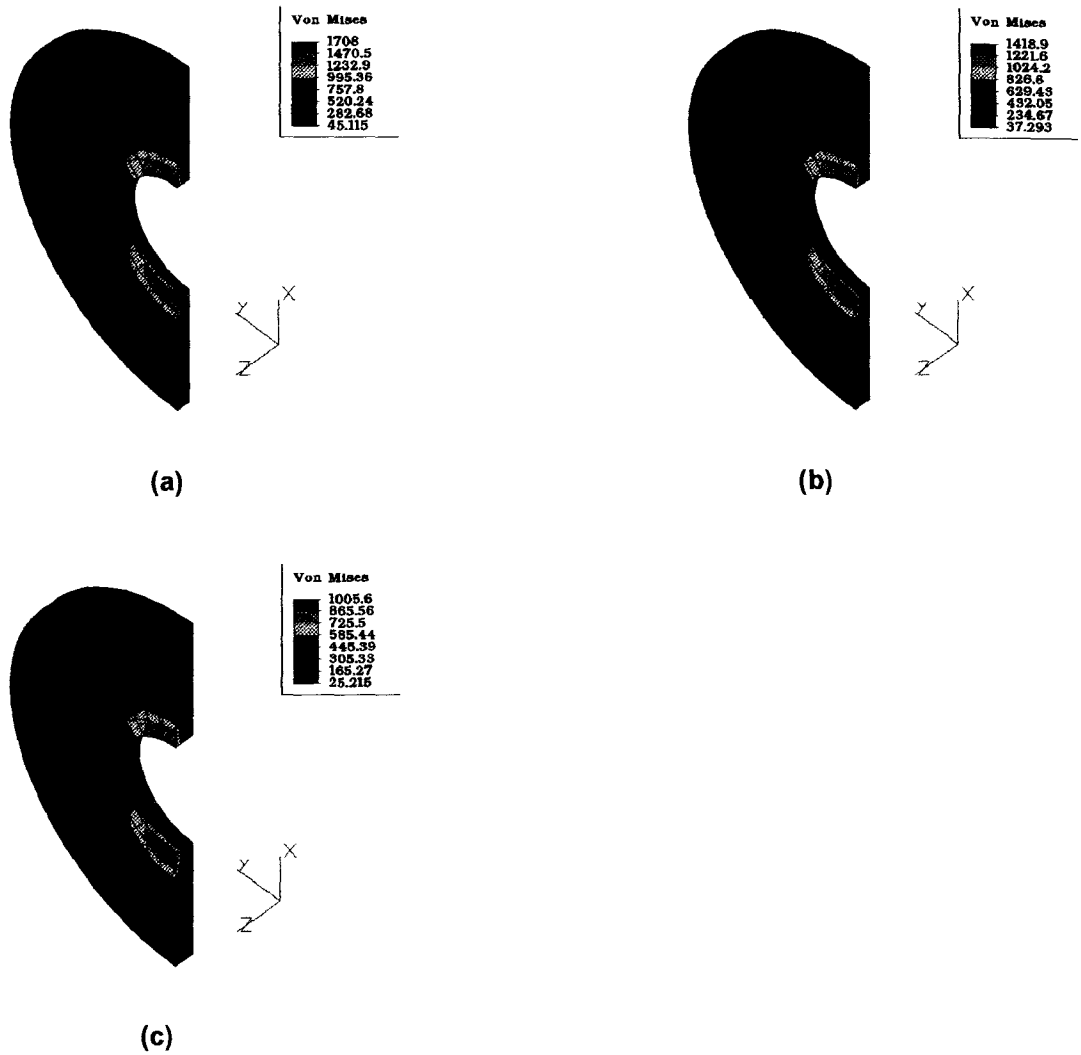

Figure 5.18 von Mises stress in the end plate of the one stiffener roll for end plate thickness of **(a)** 1", **(b)** 1¼", and **(c)** 1⅝

There was also an increase in the end plate deflection as the end plate thickness decrease from 1⅝" to 1". Figure 5.19 shows the deflection profiles for various end plate thicknesses. Notice that the scales are the same for each thickness so that again it may not be readily apparent that the profiles are actually quite similar with only a change in the absolute deflection values. The hub is also shown so that the distortion of the end plate at the end plate to hub interface can be easily identified.

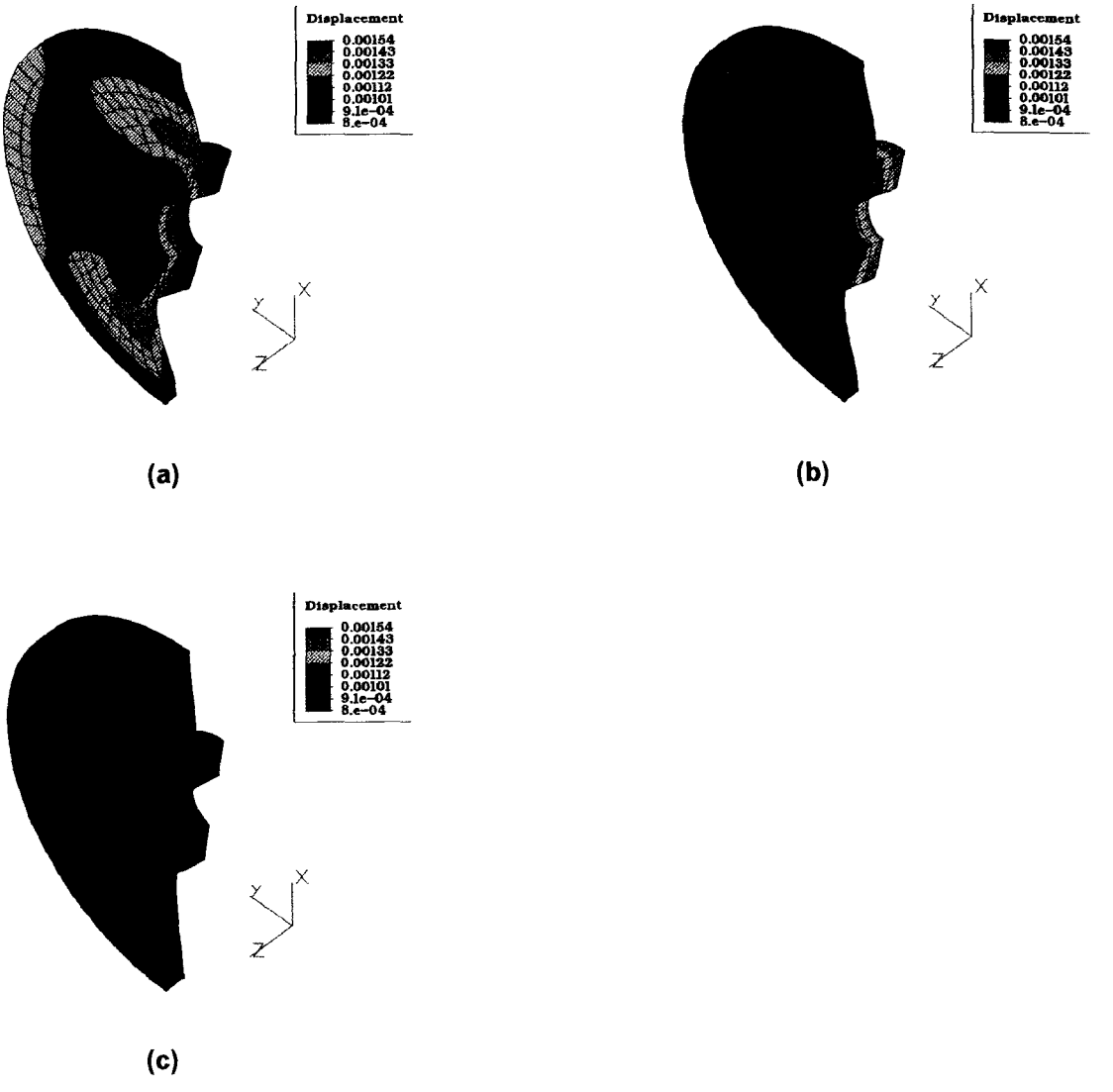

Figure 5.19 End plate deflection for the one stiffener roll for end plate thickness of **(a)** 1", **(b)** 1¼", and **(c)** 1 ⅝"

The increase in the end plate deflection was approximately 43% as the end plate thickness decreased from 1⅝" to 1". Note that just as it was determined in section 5.2 that the stress values in the end plate was independent of stiffener configuration, it was determined that end plate deflection was independent of stiffener configuration. Therefore, end plate deflection results are the same for the two stiffener and no stiffener rolls.

Table 5.4 summarizes the stresses and deflections in the roll body and the end plate for the various roll configurations considered in this section. Notice that the table shows results for end plate thicknesses that were not previously illustrated.

Table 5.4 Maximum deflection and von Mises stress as end plate thickness is varied

MODEL NAME	ROLL CONFIGURATION		MAXIMUM VON MISES		MAXIMUM DEFLECTION	
	NUMBER OF STIFFENERS	END PLATE THICKNESS	END PLATE (psi)	ROLL BODY (psi)	END PLATE (in)	ROLL BODY (in)
ads41z	2	1	1711	538	1.39E-03	1.63E-03
ads40z	2	1.125	1566	552	1.28E-03	1.56E-03
ads3z	2	1.25	1421	566	1.17E-03	1.48E-03
ads18z	2	1.375	1283	549	1.09E-03	1.43E-03
ads21z	2	1.5	1144	531	1.03E-03	1.38E-03
ads39z	2	1.625	1006	514	9.70E-04	1.33E-03
ads44z	1	1	1708	523	1.39E-03	1.65E-03
ads43z	1	1.125	1563	536	1.28E-03	1.58E-03
ads5z	1	1.25	1418	548	1.17E-03	1.50E-03
ads19z	1	1.375	1281	529	1.09E-03	1.45E-03
ads22z	1	1.5	1143	511	1.03E-03	1.39E-03
ads42z	1	1.625	1006	492	9.70E-04	1.34E-03
ads47z	0	1	1705	495	1.39E-03	1.94E-03
ads46z	0	1.125	1561.5	503	1.28E-03	1.87E-03
ads6z	0	1.25	1418	511	1.17E-03	1.79E-03
ads20z	0	1.375	1282	503	1.09E-03	1.74E-03
ads23z	0	1.5	1145	495	1.03E-03	1.69E-03
ads45z	0	1.625	1009	487	9.80E-04	1.64E-03

The last bit of information for the analysis of the end plate thickness is the deflection of the top line of nodes of the roll bodies. Figures 5.20 to 5.22 show this deflection for the two, one, and no stiffener rolls, respectively. Notice that benefit gained from increasing the thickness of the end plate diminishes as the thickness increased. This was also true when the thickness of the roll body was increased in section 5.4.

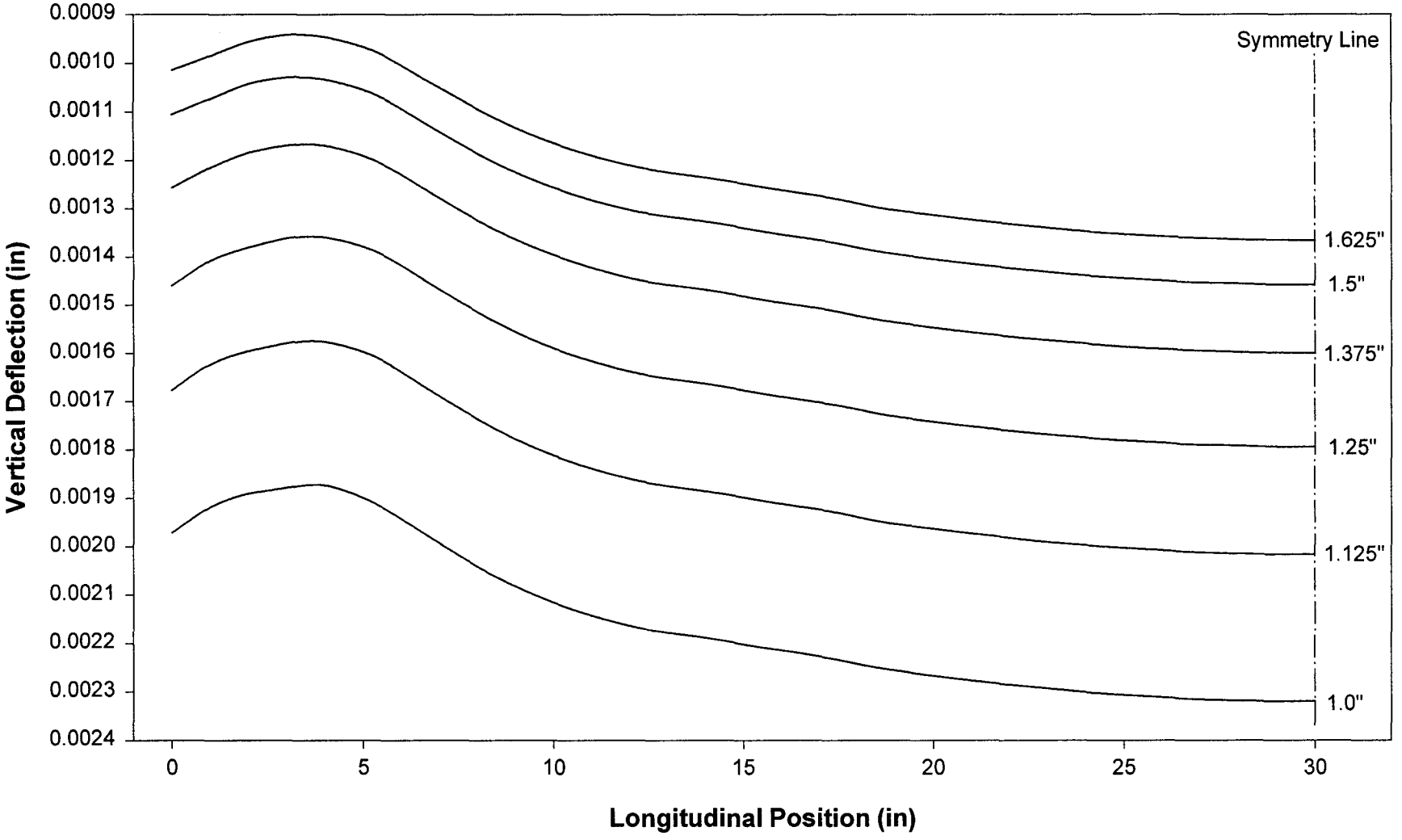

Figure 5.20 Roll body deflection with variation in end plate thickness (two stiffeners)

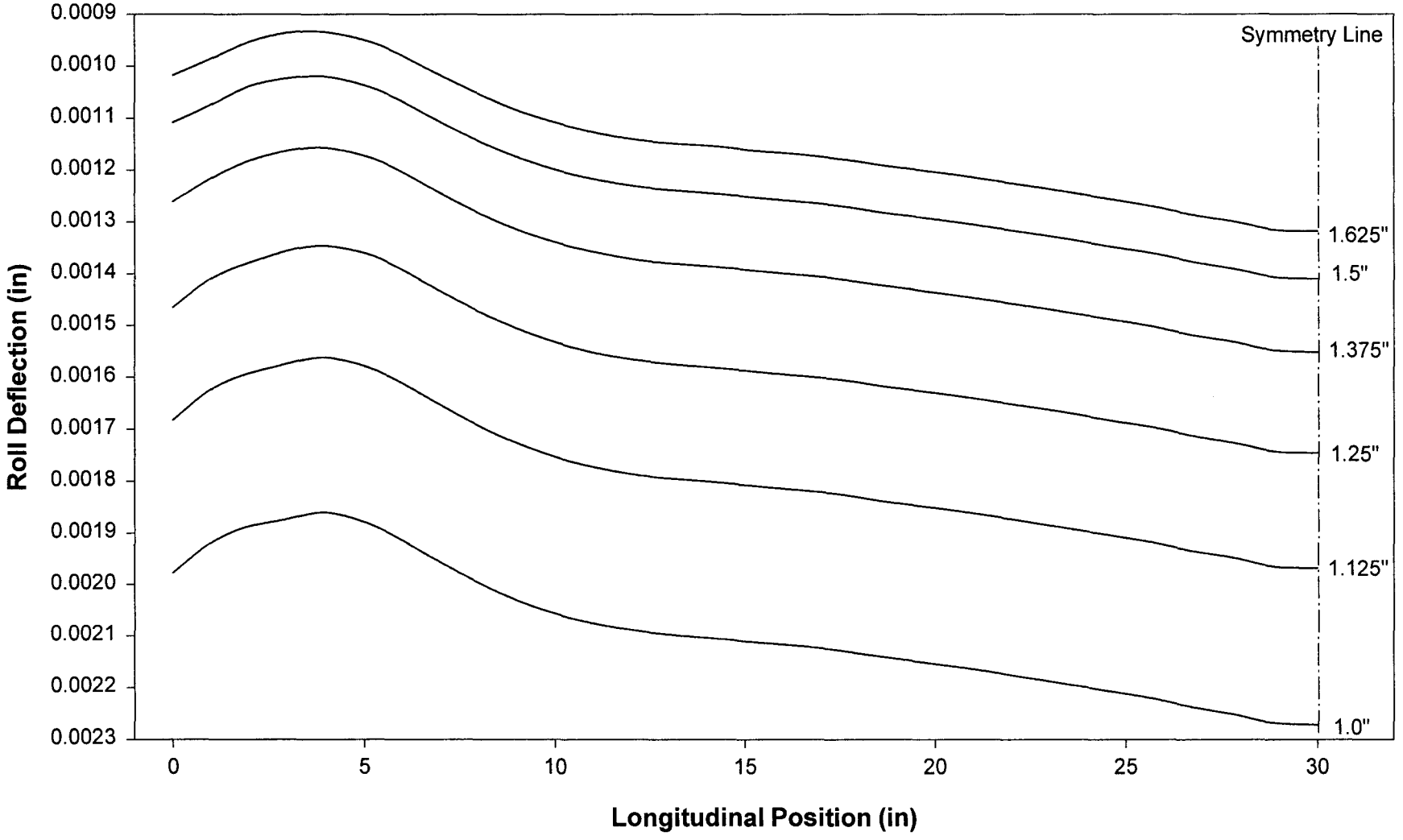

Figure 5.21 Roll body deflection with variation in end plate thickness (one stiffener)

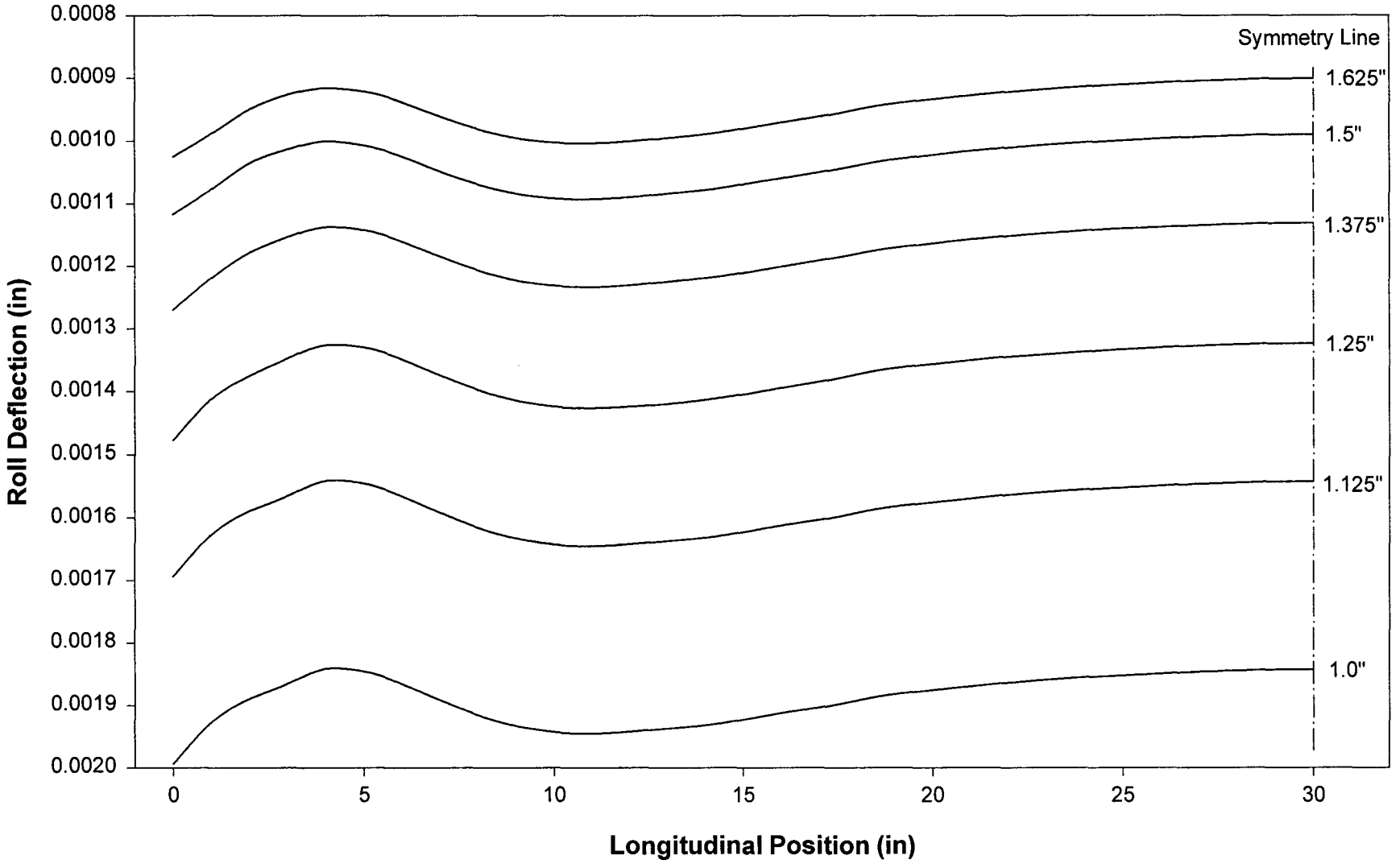

Figure 5.22 Roll body deflection with variation in end plate thickness (no stiffeners)

5.6 CONCLUSIONS

The following conclusions can be drawn from this investigation of accumulator roll design:

- Roll bodies of rolls with the original dimensions and two stiffeners located between 6" and 12" from the line of symmetry keep their circular integrity when loaded. Rolls with stiffeners located in other positions show distortion in their roll bodies.
- Thickness changes of the stiffening disks had no significant effect on the stresses in or the deflections of the entire roll.
- Changes in the roll body thickness had little effect on the end plate stresses and deflections. However, the roll body exhibited large sensitivity to a change in its thickness in terms of percentage increases in both von Mises stress and deflection. Roll body circular integrity was no longer an issue when the thickness reached 1.5" for any configuration of roll stiffeners.
- Changes in end plate thickness had significant effects only on the deflections and stresses in the end plate. Roll body stresses, deflections, and circular integrity were not significantly altered.
- The end plate had the highest stresses of the roll components at the end plate to hub connection. Therefore, caution is needed when considering a cost saving design change in this roll component.

The finite element analysis used in this investigation proved to be valuable in establishing the trend in roll stresses and deflections as different roll components were varied. Although the stress and deflection absolute values were quite small for all the design variations, the percent change in the values proved to be quite significant for some of the variations. Care therefore must be taken when considering a change that causes an increase in stress or deflection of a roll component if the applied load were higher than the one considered in this research.

REFERENCES

[1] Honeygosky,Michael A., Teofilo A. Garcia, and John A. Butine. "Finite Element Analysis of a Work Roll Chock and Roller Bearing Assembly", *Iron and Steel Engineer*, Jan. 1993.

[2] Blodgett, Omer W. Book of Weldments. Cleveland: The James F. Lincoln Arc Welding Foundation (1976)

[3] Kinnavy, M. G. "Design Considerations in Tension Leveling Systems", *Iron and Steel Engineer*, Oct. 1990.

[4] Sheppard, T. and J. M. Roberts. "On the Strip-to-Roll Conformity in the Tension-Leveling Process." Journal of the Institute of Metals. Vol.100 (1972): 130-135.

[5] Avallone, Eugene A. and Theodore Baumeister III, ed. Marks' Standard Handbook for Mechanical Engineers. New York: McGraw-Hill, 1996

[6] "Algor Users Manual", Algor Docutech Version 2.14, Algor Inc., 1996.

[7] "ALGOR Elements Reference", Algor Docutech Version 2.14, Algor Inc., 1996.

APPENDEX

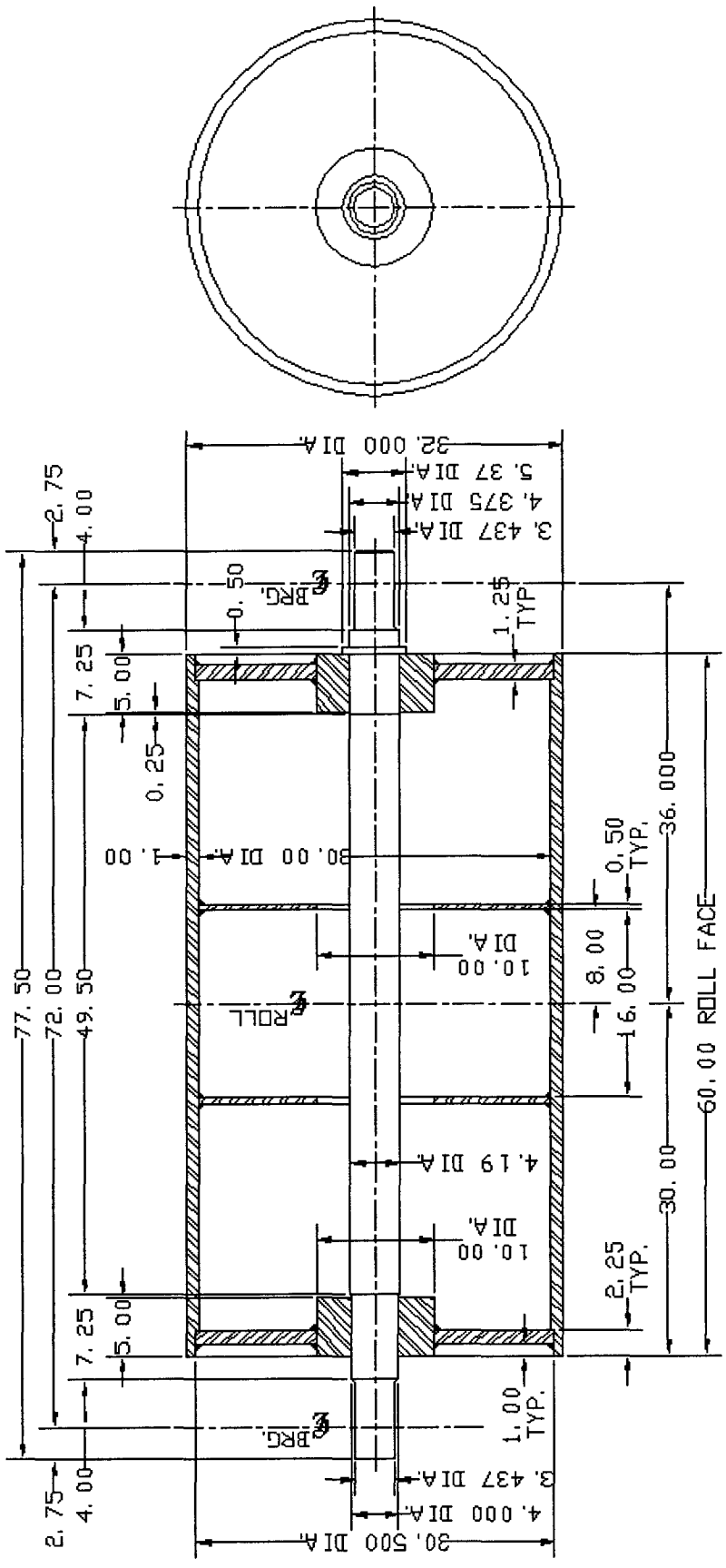

Figure A.1 Schematic of original roll investigated in this research

Table A.1 Configuration of models investigated in this research

MODEL NAME	DEVIATION FROM ORIGINAL ROLL				
	STIFFENER NUMBER	STIFFENER LOCATION	STIFFENER THICKNESS	ROLL BODY THICKNESS	END PLATE THICKNESS
original	2	8.25	0.50	1.00	1.25
ads3z					
ads7z1		10.25			
ads7z2		12.25			
ads7z3		14.25			
ads7z4		16.25			
ads7z5		6.25			
ads7z6		4.00			
ads8z1			0.25		
ads8z			0.75		
ads10z			1.00		
ads12z				1.13	
ads15z				1.25	
ads24z				0.75	
ads27z				0.50	
ads30z				1.50	
ads33z				1.75	
ads36z				2.00	
ads18z					1.38
ads21z					1.50
ads39z					1.63
ads40z					1.13
ads41z					1.00
ads5z	1	0.00			
ads9z1	1	0.00	0.25		
ads9z	1	0.00	0.75		
ads11z	1	0.00	1.00		
ads13z	1	0.00		1.13	
ads16z	1	0.00		1.25	
ads25z	1	0.00		0.75	
ads28z	1	0.00		0.50	
ads31z	1	0.00		1.50	
ads34z	1	0.00		1.75	
ads37z	1	0.00		2.00	
ads19z	1	0.00			1.38
ads22z	1	0.00			1.50
ads42z	1	0.00			1.63
ads43z	1	0.00			1.13
ads44z	1	0.00			1.00
ads6z	0				
ads14z	0			1.13	
ads17z	0			1.25	
ads26z	0			0.75	
ads29z	0			0.50	
ads32z	0			1.50	
ads35z	0			1.75	
ads38z	0			2.00	
ads20z	0				1.38
ads23z	0				1.50
ads45z	0				1.63
ads46z	0				1.13
ads47z	0				1.00